*Zootaxa* 5897 (4): 343–375
https://www.mapress.com/zt/
Copyright © 2026 Magnolia Press

**Article**

ISSN 1175-5326 (print edition)
**ZOOTAXA**
ISSN 1175-5334 (online edition)

https://doi.org/10.11646/zootaxa.5897.4.2
http://zoobank.org/urn:lsid:zoobank.org:pub:8897FB84-FF75-43E6-A382-FEF8B05116F8

# At the western edge of South Asia: a new species of *Eremias* Fitzinger, 1834 (Squamata: Lacertidae) from Balochistan and confirmed records of *E. fasciata* Blanford, 1874 for Pakistan

RAFAQAT MASROOR[1]*, MUHAMMAD DANISH[2] & DANIEL JABLONSKI[3,4]*

[1]*Zoological Sciences Division, Pakistan Museum of Natural History, Garden Avenue, Shakarparian, Islamabad-44000, Pakistan.*
[2]*Biodiversity Officer, Reko Diq Mining Company, Quetta, Balochistan, Pakistan.*
*muhammad.danish@rekodiqmc.com;* *https://orcid.org/0009-0008-2252-2287*
[3]*Department of Zoology, Comenius University in Bratislava, Ilkovičova 6, Mlynská dolina, 842 15, Bratislava, Slovakia.*
[4]*Herpetological Collection, 1st Zoological Department, Natural History Museum Vienna, Burgring 7, 1010 Vienna, Austria.*
*daniel.jablonski@uniba.sk;* *https://orcid.org/0000-0002-5394-0114*
*rafaqat.masroor78@gmail.com;* *https://orcid.org/0000-0001-6248-546X*
**Corresponding authors.*

## Abstract

We discovered a previously unrecognized evolutionary lineage of *Eremias* assigned to the subgenus *Rhabderemias* in the Pakistan–Afghanistan border region. Although superficially similar to the recently described Iranian species *E. graphica* in its vermiculate dorsal pattern, mitochondrial phylogenetic analyses recover this lineage as sister to *E. fasciata*, while nuclear DNA data independently support its distinctiveness. The new lineage was recorded from low, mobile sand dunes in northwestern Balochistan, Pakistan, at the southeastern margin of the Registan Desert. It is clearly differentiated from *E. fasciata* by both mitochondrial and nuclear markers, with mean uncorrected *p*-distances of approximately 10.6% for mitochondrial DNA and 0.9% for nuclear DNA. Morphologically, it differs from most species traditionally assigned to *Rhabderemias* in retaining a vermiculate dorsal pattern in both juveniles and adults rather than the longitudinally striped pattern characteristic of the group. It is further distinguished from *E. graphica* and the sympatric *E. fasciata* by a combination of dorsal coloration, scalation, body proportions, and habitat association, with multivariate morphological analyses supporting its distinctiveness from both species. Given the continuity of suitable sandy habitats across international borders, the new species is likely to occur more widely within the Registan Desert of southwestern Afghanistan and possibly adjacent eastern Iran. Our integrative analyses also provide the first definitive confirmation of the long-debated occurrence of *E. fasciata* in Pakistan. These findings increase the known diversity of *Rhabderemias* to 12 species, five of which occur in Pakistan, and bring the total number of *Eremias* species recorded from the country to eight.

**Key words:** Palearctic, *Rhabderemias*, endemism, new species, Lacertidae

## Introduction

The genus *Eremias* Fitzinger, 1834 belongs to the tribe Eremiadini (Arnold 1989) and currently encompasses 44 recognized species occupying a wide range of steppe, desert, and montane ecosystems across the Eurasian landmass (Uetz *et al.* 2026). Its distribution extends from the Korean Peninsula westward through China and Mongolia, across Central and South Asia and the Middle East, reaching into Romania in eastern Europe (Sindaco & Jeremčenko 2008; Rastegar-Pouyani *et al.* 2010; Guo *et al.* 2011; Orlova *et al.* 2017). Based on distinctive external morphology and hemipenial structure, the genus is subdivided into five subgenera: *Eremias* Fitzinger, 1834; *Rhabderemias* Lantz, 1928; *Aspidorhinus* Eichwald, 1841; *Scapteira* Fitzinger, 1834; and *Pareremias* Szczerbak, 1973 (Arnold 1986; Ananjeva *et al*. 1998; Chirikova 2004; Barabanov 2009; Guo *et al.* 2010), although their taxonomic boundaries require further evaluation.

Although the group has been the focus of numerous studies addressing its distribution, taxonomy, phylogeny, and phylogeography (e.g. Szczerbak 1971, 1974; Guo *et al.* 2011; Orlova *et al.* 2017; Khan *et al*. 2021), species diversity within *Eremias* remains insufficiently resolved, especially from poorly investigated territories. Recent

*Accepted by J. Šmíd: 2 Oct. 2026; published: 3 Nov. 2026*

DNA-based studies, however, have led to the recognition of several new species from Iran and broader Central Asia, underscoring the likelihood of additional undocumented diversity (e.g. Rastegar-Pouyani *et al.* 2016; Masroor *et al.* 2020a, 2022; Orlova *et al.* 2017, 2023).

In Pakistan, seven species of *Eremias* have been recorded to date (see Baig & Masroor 2006; Masroor *et al*. 2020a, 2022; Khan *et al.* 2021). The specimen reported traditionally as *E. persica* from western Pakistan by Minton (1966: pl. 22) and Mertens (1969) belongs to the recently described *E. rafiqi* Masroor, Khan, Nadeem, Amir, Khisroon & Jablonski, 2022, whereas *E. persica* sensu stricto is probably absent from Pakistan. These taxa are distributed primarily across the arid and submontane regions of southwestern, central, and eastern Pakistan and represent three subgenera: *Aspidorhinus* (two species), *Rhabderemias* (four species), and *Scapteira* (one species) (Khan *et al.* 2021; Masroor *et al.* 2022). Most Pakistani representatives of *Scapteira* and *Rhabderemias* are restricted to sandy dune habitats in the Nushki and Chagai districts along the Pakistan–Afghanistan border. One species, *E. cholistanica* Baig & Masroor, 2006, apparently evolved east of the Indus Valley and is now endemic to the Cholistan Desert along the Pakistan–India border. Members of *Aspidorhinus*, including *E. killasaifullahi* Masroor *et al.* 2022 and *E. rafiqi* Masroor *et al.* 2022, inhabit the dry mountain systems of northwestern Balochistan. The occurrence of *E. fasciata* Blanford, 1874 in Pakistan is more enigmatic. Although the species was reported from southwestern Balochistan by Boulenger (1921), its presence in the country has not subsequently been confirmed (Lantz 1928; Smith 1935; Minton 1966; Mertens 1969; Khan & Ahmed 1987). Owing to the high diversity of morphologically similar lacertid lizards in the region and the limited accessibility of large parts of Balochistan, its status in Pakistan has therefore remained unresolved.

Recent work in neighbouring India has revealed substantial hidden diversity in open-habitat lacertids (Agarwal & Ramakrishnan 2017; Agarwal *et al.* 2018), whereas the lacertid fauna of Pakistan remains comparatively less explored. In this context, the present study aimed to assess lacertid diversity in northwestern Balochistan. During field surveys conducted in April and May 2025 in northwestern Chagai District, we collected specimens exhibiting a distinct vermiculate dorsal pattern in both juveniles and adults and possessing a combination of morphological traits that clearly distinguish them from previously described congeners within the subgenus *Rhabderemias*. Preliminary identification based on standard taxonomic keys (Minton 1966; Anderson 1999; Rastegar-Pouyani *et al.* 2016; Orlova *et al.* 2023) indicated that this population represents an undescribed species within the subgenus *Rhabderemias*, warranting formal taxonomic description.

## Materials and methods

### DNA laboratory

Genomic DNA was extracted from blood and muscles using E.Z.N.A.® Tissue DNA Kit, following the manufacturer's protocol. The material analysed genetically comprised the eight specimens of the type series (see below) and two additional samples (DJ13875; DJ13897 collected on 7 and 9 May 2025 from 29.5979°N, 61.5125°E and 29.2563°N, 61.8969°E, respectively) of the newly discovered lineage, and three Pakistani specimens of *E. fasciata* (PMNH 5083, PMNH 5066, and DJ13825). Three protein-coding loci were targeted: the mitochondrial cytochrome c oxidase subunit I (COI) and cytochrome *b* (cyt *b*) genes, and the nuclear recombination-activating gene 1 (Rag-1).

An approximately 655-bp fragment of COI was amplified using the primers VF1-d (5′-TTCTCAACCAACCACAARGAYATYGG-3′) and VR1-d (5′-TAGACTTCTGGGTGGCCRAARAAYCA-3′), developed by Ivanova *et al*. (2007). Cytochrome *b* was amplified using the forward primer LgluLK (5′-AACCGCTGTTGTCTTCAACTA-3′; Pavlicev & Mayer 2009) and the reverse primer Lacertidae_cytb (5′-AAARTTTTCTGGGTCSCCKA-3′; Khan *et al.* 2021). Rag-1 was amplified using the primers R13 (5′-TCTGAATGGAAATTCAAGCTGTT-3′) and R18 (5′-GATGCTGCCTCGGTCGGCCACCTTT-3′), described by Groth & Barrowclough (1999).

PCRs were performed in total volumes of 20 µl containing approximately 20 ng of template DNA and Red Taq 2× Master Mix with $MgCl_2$. For reactions showing weak amplification, 0.25 µl of 100 mM $MgCl_2$ was added to the reaction mixture. For COI, the thermal profile consisted of an initial denaturation at 95 °C for 2 min, followed by 40 cycles of denaturation at 95 °C for 40 s, annealing at 50 °C for 30 s, and extension at 72 °C for 60 s, with a final extension at 72 °C for 7 min. For cyt *b*, the thermal profile consisted of an initial denaturation at 95 °C for 2 min, followed by 35 cycles of denaturation at 95 °C for 35 s, annealing at 50 °C for 35 s, and extension at 72 °C for 60 s,

with a final extension at 72 °C for 7 min. For Rag-1, the thermal profile consisted of an initial denaturation at 95 °C for 2 min, followed by 39 cycles of denaturation at 95 °C for 40 s, annealing at 58–63 °C for 30 s, and extension at 72 °C for 60 s, with a final extension at 72 °C for 10 min.

PCR products were purified enzymatically using ExoSAP-IT PCR Product Cleanup Reagent (Applied Biosystems, Foster City, CA, USA), diluted 1:20. Purification consisted of incubation at 37 °C for 30 min, followed by enzyme inactivation at 80 °C for 15 min. Purified amplicons were sequenced bidirectionally using Sanger sequencing by Macrogen Europe B.V. (Amsterdam, the Netherlands). The corresponding amplification primers were also used for cycle sequencing of COI, cyt *b*, and Rag-1.

## Genetic data and analyses

Forward and reverse reads were inspected, assembled into consensus sequences, and manually edited. Low-quality terminal regions were trimmed, and ambiguous nucleotide calls were resolved by comparison of complementary reads. Sequences were aligned separately for each locus in SeaView 5 (Gouy *et al.* 2021) under default settings. Because analysed genes are protein-coding loci, the alignments were translated into amino acids to verify the reading frame and screen for premature stop codons, frameshifts, and unexpected insertions or deletions. The vertebrate mitochondrial genetic code was used for COI and cyt *b*, whereas the standard nuclear genetic code was used for Rag-1. Comparative sequences for final alignments were retrieved from GenBank and are shown on Figs. 1, 2C and 3 as well as listed in Appendix 1. New sequences were deposited in GenBank under accession numbers PZ987599-PZ987611 (COI), QB002726-QB002738 (cyt *b*), and QB002365-QB002372 (Rag-1).

To assess species identity and phylogenetic placement, maximum-likelihood (ML) analyses of the COI and cyt *b* datasets were conducted separately in IQ-TREE v. 3.0.1 (Wong *et al.* 2026). The two mitochondrial markers were analyzed separately because specimen and taxon coverage differed substantially between datasets. Concatenation restricted to samples represented by both markers would have markedly reduced taxon sampling, whereas inclusion of all available samples in a concatenated matrix would have introduced extensive missing data for one of the loci. As both markers are mitochondrial and physically linked, the resulting trees were not treated as independent evolutionary histories. The final COI dataset comprised 107 sequences and 657 aligned nucleotide positions, whereas the cyt *b* dataset comprised 25 sequences and 751 aligned positions. Each protein-coding alignment was partitioned according to codon position, and an edge-linked proportional partition model was applied (Chernomor *et al.* 2016). For COI, the optimal partitioning scheme and best-fitting nucleotide-substitution models were selected using ModelFinder Plus with partition merging (MFP+MERGE) under the Bayesian information criterion (BIC; Kalyaanamoorthy *et al.* 2017). All three codon-position partitions were retained, with TN+I+G4, F81+F+R2, and TN+F+G4 selected for the first, second, and third codon positions, respectively. For cyt *b*, substitution models were selected independently for the three predefined codon-position partitions under the BIC, without partition merging. The selected models were TIM2+G4, HKY+F+I, and TN+F+I+G4 for the first, second, and third codon positions, respectively. ML tree searches were performed using the default IQ-TREE settings. Nodal support was evaluated using 1,000 replicates of the Shimodaira–Hasegawa-like approximate likelihood-ratio test (SH-aLRT; Guindon *et al.* 2010) and 1,000 ultrafast bootstrap replicates (UFBoot2; Hoang *et al.* 2018).

Bayesian inference analyses (BI) were also performed separately in MrBayes v3.2 (Ronquist *et al.* 2012), using the same dataset and three codon-position partitions as in the ML analyses. For each partition, a mixed reversible substitution model with gamma-distributed among-site rate variation was used, with substitution parameters unlinked among partitions and relative partition rates allowed to vary. Two independent runs, each with four Markov chains, were conducted for 10 million generations, sampling every 1,000 generations. The first 25% of samples were discarded as burn-in. Convergence was assessed using the average standard deviation of split frequencies and potential scale reduction factors (PSRF) reported by MrBayes, and effective sample sizes (ESS > 200) were verified in Tracer v1.7 (Rambaut *et al*. 2018). The final average standard deviation of split frequencies was 0.0058 for COI and 0.0026 for cyt *b*.

Nodal support is reported as SH-aLRT/UFBoot/BI posterior probability (PP). Nodes meeting both ML thresholds of SH-aLRT ≥80% and UFBoot ≥95% were considered strongly supported.

The nuclear Rag-1 dataset was analysed within a haplotype framework to account for allele-level variation characteristic of a diploid marker. The final alignment comprised nine unphased diploid sequences and 990 aligned

nucleotide positions. Heterozygous sites were coded using the corresponding IUPAC ambiguity symbols. Allelic phase was inferred using the PHASE algorithm (Stephens *et al.* 2001), as implemented in Hapsolutely (Vences *et al.* 2024b), with default settings. Phasing yielded 18 allelic sequences representing seven distinct Rag-1 haplotypes. Relationships among the phased haplotypes were reconstructed and visualized in Hapsolutely using the TCS statistical-parsimony approach, with node sizes proportional to haplotype frequencies. The resulting nuclear pattern was interpreted together with the independently inferred mitochondrial COI and cyt *b* data to assess allele sharing and concordance among loci. For comparison, mitochondrial COI (n = 13; 607 bp) and cyt *b* (n = 12; 751 bp) haplotype networks were also reconstructed and visualized in Hapsolutely using the TCS statistical-parsimony approach.

Uncorrected p-distances were calculated separately for each gene in DnaSP 6 (Rozas *et al*. 2017). Distribution maps were prepared in QGIS v. 3.44 Solothurn (QGIS Development Team 2025). Extent of occurrence (EOO) was calculated using a minimum convex polygon, whereas area of occupancy (AOO) was calculated using a standard 2 × 2 km grid.

## Morphological data and analyses

The eight collected specimens of the newly revealed lineage and eight specimens of *E. fasciata* (see Table 1 and 2) deposited in the Pakistan Museum of Natural History, Islamabad, Pakistan (PMNH) and Natural History Museum Vienna (NHMW) were examined for 45 morphological characters by recording their mensural, meristic and qualitative data, following Boulenger (1890, 1918, 1921), Lantz (1928), Szczerbak (1974), Rastegar-Pouyani *et al.* (2016), Orlova *et al.* (2017) and Masroor *et al.* (2020a). All measurements were carried out to the nearest 0.01 mm by using a digital vernier caliper by the first author (RM). The scales were counted with the use of a stereomicroscope. Measurements of arms, legs, and head as well as scale counts beneath the toes were principally taken on the right side of the specimens.

We recorded the following morphological characters: **SVL** (snout-vent length, from the tip of snout to the anterior edge of the cloaca); **TL** (tail length, from the posterior edge of cloaca to the tip of the tail); **TrL** (trunk length, the distance from axilla to groin measured from posterior edge of forelimb insertion to anterior edge of hindlimb insertion); **HL** (head length, distance between snout-tip and retroarticular process of jaw); **Lpil** (length of pileus, from rostrum to the posterior border of parietals); **NL** (snout-to-collar length, measured ventrally from the tip of the snout to the anterior edge of the collar); **HW** (head width, measuring widest part of the head); **HH** (head height, from occiput to underside of jaws); **FrL** (length of frontal scale); **FrW** (maximum width of frontal scale); **SNL** (length of the supranasal suture); **FNL** (length of frontonasal); **PFL** (length of prefrontal); **PFW** (width of prefrontal); **HLL** (hindlimb length, from hindlimb insertion to the tip of the longest toe); **FLL** (forelimb length, from forelimb insertion to the tip of the longest finger); **HRL** (length of humerus and radius, from forelimb insertion to palm, excluding the digits); **FL** (femur length, from hindlimb insertion to knee); **CL** (Crus length or tibia length, from the base of the heel to knee); **LFPR** (length of femoral pore row); **LFPS** (width of space between femoral pore rows); **SL** (supralabials, counted on both right and left sides); **SLAS** (number of supralabials anterior to subocular, counted on both right and left sides); **IL** (infralabials, counted on both right and left sides); **G** (gulars, from chin shields to the collar); **Coll** (number of enlarged collar scales); **Submax** (number of submaxillary shields); **Supracil** (number of supraciliars, right/left); **DS** (number of dorsal scales on midbody); **SqDors** (number of dorsal scales between parietals and the level of cloaca); **VL** (maximum number of scales across mid-belly in a single row in the widest part); **VT** (number of ventral scales in a single row from posterior edge of collar to the vent); **FP** (number of femoral pores, counted on both right and left sides); **FPS** (number of scales separating femoral pore rows); **SDLT 4$^{th}$** (subdigital lamellae under 4$^{th}$ toe); **SAT 4$^{th}$** (number of scales around 4$^{th}$ toe at the penultimate phalanx); **SDLF 4$^{th}$** (subdigital lamellae under 4$^{th}$ finger); **NCWS** (scales around ninth and tenth caudal whorl posterior to the vent); **FMIL** (contact of fifth maxillary/chin shield with infralabial; in contact (+)/separated (-)); **SOM** (subocular in contact with mouth; present (+)/absent (-)); **FSO** (contact of frontal and supraoculars; in contact (+)/separated (-)); **INTR** (contact of infranasal with rostral; in contact (+)/separated (-)); **Gran** (supraocular separated from frontal and frontoparietal by a complete row of small granular scales, presence (+)/absent (-)); **LB** (dorsal longitudinal dark bands, present (+)/absent (-)) and **FSpots** (roundish light spots on the femur, present (+)/absent (-)).

For morphological comparisons with species from the subgenus *Rhabderemias*, we checked available morphological data of original descriptions as well as other relevant publications (Kessler 1878; Nikolsky 1896;

Bedriaga 1907; Nikolsky 1915; Lantz 1928; Minton 1966; Anderson & Leviton 1967; Başoğlu & Hellmich 1968; Szczerbak 1972; Bischoff & Böhme 1980; Szczerbak 1981; Böhme & Szczerbak 1991; Moravec 1994; Rastegar-Pouyani & Nilson 1997; Anderson 1999; Rastegar-Pouyani & Rastegar-Pouyani 2001; Baig & Masroor 2006; Mozaffari *et al.* 2011, 2020; Rastegar-Pouyani *et al.* 2016; Masroor *et al.* 2020a; see Appendix 2).

Morphological differentiation among phylogenetically and/or morphologically closely related *E. fasciata*, *E. graphica* and the newly discovered lineage was assessed using MFA (Grismer 2025) in GroupStruct2 v1.3.1 (Chan & Grismer 2026). Only characters scored for all specimens were included, and no missing values were imputed. The final dataset comprised 26 specimens (*E. fasciata*, n = 8; *E. graphica*, n = 10; new lineage, n = 8). Data for *E. graphica* were taken from Orlova *et al*. (2023).

Two quantitative data blocks were analyzed. The morphometric block comprised Lpil, HL, HW, HH, TrL, FLL, and HLL. Tail length and tail-derived ratios were excluded because some specimens had broken or regenerated tails. The meristic block comprised DS, G, FPS, VL, VT, NCWS, SDLT4, SqDors, FP, SL, IL, and Supracil. For bilateral characters (FP, SL, IL, and Supracil), right and left counts were averaged; where only a single value was recorded, that value was retained. Invariant and incompletely scored characters were excluded.

Morphometric variables were subjected to the multispecies allometric correction using SVL as the body-size variable. The correction was applied only to the seven morphometric traits. Size-corrected, log-transformed morphometric variables and the original meristic variables were then analyzed as separate MFA blocks. Eigenvalues and contributions of data blocks and individual variables were used to characterize the principal MFA dimensions.

Differences among taxa were tested by PERMANOVA using Euclidean distances calculated from all retained MFA dimensions and 10,000 permutations, followed by pairwise comparisons. Homogeneity of multivariate dispersion was assessed using betadisper with 10,000 permutations. Morphological group structure was additionally explored using Gaussian mixture modelling (GMM) of MFA scores. A threshold-sensitivity analysis was first performed, and the final clustering retained the first four MFA dimensions (76.5% cumulative variance). The maximum number of clusters was set to three, corresponding to the three taxa examined, and the optimal model was selected according to the Bayesian Information Criterion (BIC). Cluster assignments were subsequently compared with the original identifications.

Boxplots were used to visualize six meristic characters (DS, SqDors, FP, G, NCWS, and SDLT4) that contributed substantially to the first two MFA dimensions and showed clear interspecific variation.

## Results

### Mitochondrial differentiation

The COI phylogeny recovered the focal Pakistani specimens in two distinct, reciprocally monophyletic lineages (Fig. 1A, B), with congruent relationships in the ML and BI analyses. Specimens PMNH 5083, PMNH 5066, and DJ13825 were nested among previously published sequences of *E. fasciata*, forming a strongly supported lineage (97.7/99/1.00; SH-aLRT/UFBoot/PP). All examined specimens of the newly discovered Chagai lineage formed a strongly supported clade (99.7/100/1.00). This lineage was recovered as sister to *E. fasciata*, with moderate ML support and a Bayesian posterior probability of 0.86 (69.1/93/0.86). The lineage comprising *E. fasciata* and the Chagai lineage was, in turn, sister to sequence OR268285.1, identified as *E.* cf. *fasciata* (72.7/92/0.97). Mean uncorrected COI *p*-distance between *E. fasciata* and the Chagai lineage was 10.6% (range 10.5–11.0%), whereas genetic variation within the new lineage was low (mean 0.10%, maximum 0.49%).

The cyt *b* phylogeny recovered the same focal relationships in both ML and BI analyses (Fig. 1C). The Chagai lineage formed a monophyletic group with strong support (90.2/95/1.00). Specimens PMNH 5083, PMNH 5066, and DJ13825 formed a strongly supported *E. fasciata* lineage (99.5/99/1.00). These two lineages were again recovered as sister lineages (89.5/87/0.98). Mean uncorrected cyt *b* *p*-distance between *E. fasciata* and the Chagai lineage was 10.6% (range 10.4–10.7%), whereas genetic variation within the Chagai lineage was low (mean 0.07%, maximum 0.27%). Thus, both mitochondrial markers consistently recovered the Chagai lineage as a genetically cohesive lineage distinct from, and sister to, *E. fasciata*, with the focal relationships congruent between ML and BI analyses.

The haplotype networks were congruent with tree analyses and showed complete haplotype segregation between *E. fasciata* and the new lineage (Fig. 3). In the COI network (607 bp), the two species were separated by a long

branch corresponding to 64 mutational steps. *Eremias fasciata* comprised two closely related haplotypes, one shared by PMNH 5083 and PMNH 5066 and the other represented by DJ13825, whereas all analysed specimens of the Chagai lineage shared a single haplotype.

The cyt *b* network (751 bp) showed an even deeper separation, with the haplotype groups of the two species separated by 78 mutational steps (Fig. 3). Three closely related haplotypes were recovered within the Chagai lineage. The predominant haplotype was shared by seven specimens, a second haplotype was represented by PMNH 5174, and a third was shared by PMNH 5173 and DJ13875. The two analysed specimens of *E. fasciata*, DJ13825 and PMNH 5083 (PMNH 5066 is shorter fragment and thus removed from this analysis), represented distinct haplotypes.

## Nuclear differentiation

The nuclear Rag-1 network (990 bp) likewise showed no allele sharing between *E. fasciata* and the new lineage, implying that both lineages are well separated (Fig. 3). Several closely related alleles were recovered within the new lineage, including alternative equally parsimonious connections involving the phased alleles of NHMW-Zoo-HS-42337:1 and DJ13897. *Eremias fasciata* was represented by a distinct allele of DJ13825. Mean uncorrected Rag-1 p-distance between *E. fasciata* and the Chagai lineage was 0.91% (range 0.81–1.01%), whereas genetic variation within the Chagai lineage was low (mean 0.20%).

## Morphological differentiation

The first two MFA dimensions explained 60.42% of the total variation (Dim1 = 35.46%, Dim2 = 24.96%) and showed clear separation of *E. fasciata*, *E. graphica* and the new lineage in the ordination space (Fig. 4A). Both data blocks contributed substantially to the main dimensions, with meristic characters contributing more to Dim1 and morphometric characters more to Dim2. The highest contributions to Dim1 were from Lpil, HL, HW, HH, DS, and SqDors, whereas Dim2 was dominated by HLL and FLL, followed by FPS and NCWS (Fig. 4B).

PERMANOVA on MFA scores showed significant morphological differentiation among the three taxa ($F_{2,23}$ = 11.71, $R^2$ = 0.504, $p < 0.001$). Pairwise comparisons were significant for all taxon pairs, with the strongest differentiation between the new lineage and *E. fasciata* (F = 17.07, $R^2$ = 0.549, p = 0.0003), followed by new lineage and *E. graphica* (F = 11.07, $R^2$ = 0.409, p = 0.0001), and *E. fasciata* and *E. graphica* (F = 8.61, $R^2$ = 0.350, p = 0.0001). Multivariate dispersion did not differ significantly among taxa ($F_{2,23}$ = 1.18, p = 0.330), and all pairwise dispersion tests were non-significant.

Unsupervised Gaussian mixture modelling recovered three clusters that corresponded exactly to the three taxonomic groups, with all specimens assigned to the cluster matching their taxonomic identification. Variation in selected meristic characters (DS, SqDors, FP, G, NCWS, and SDLT4) was further illustrated by boxplots (Fig. 4C).

## Taxonomic implications

Following the General Lineage Concept (GLC), we regard species as separately evolving metapopulation lineages and assess their status using multiple operational criteria within an integrative taxonomic framework (de Queiroz 2007; Dufresnes *et al.* 2023; Vences *et al.* 2024a). The Chagai lineage is consistently differentiated from *E. fasciata* in mitochondrial DNA and the sampled nuclear Rag-1 marker and is further characterized by a diagnosable phenotype and a geographically coherent distribution. The concordance among mitochondrial, nuclear, morphological, and geographic evidence supports its interpretation as a separately evolving species-level lineage. Its recognition is therefore based on the cumulative evidence for lineage differentiation and evolutionary independence. We consequently describe the Chagai lineage herein as a new species.

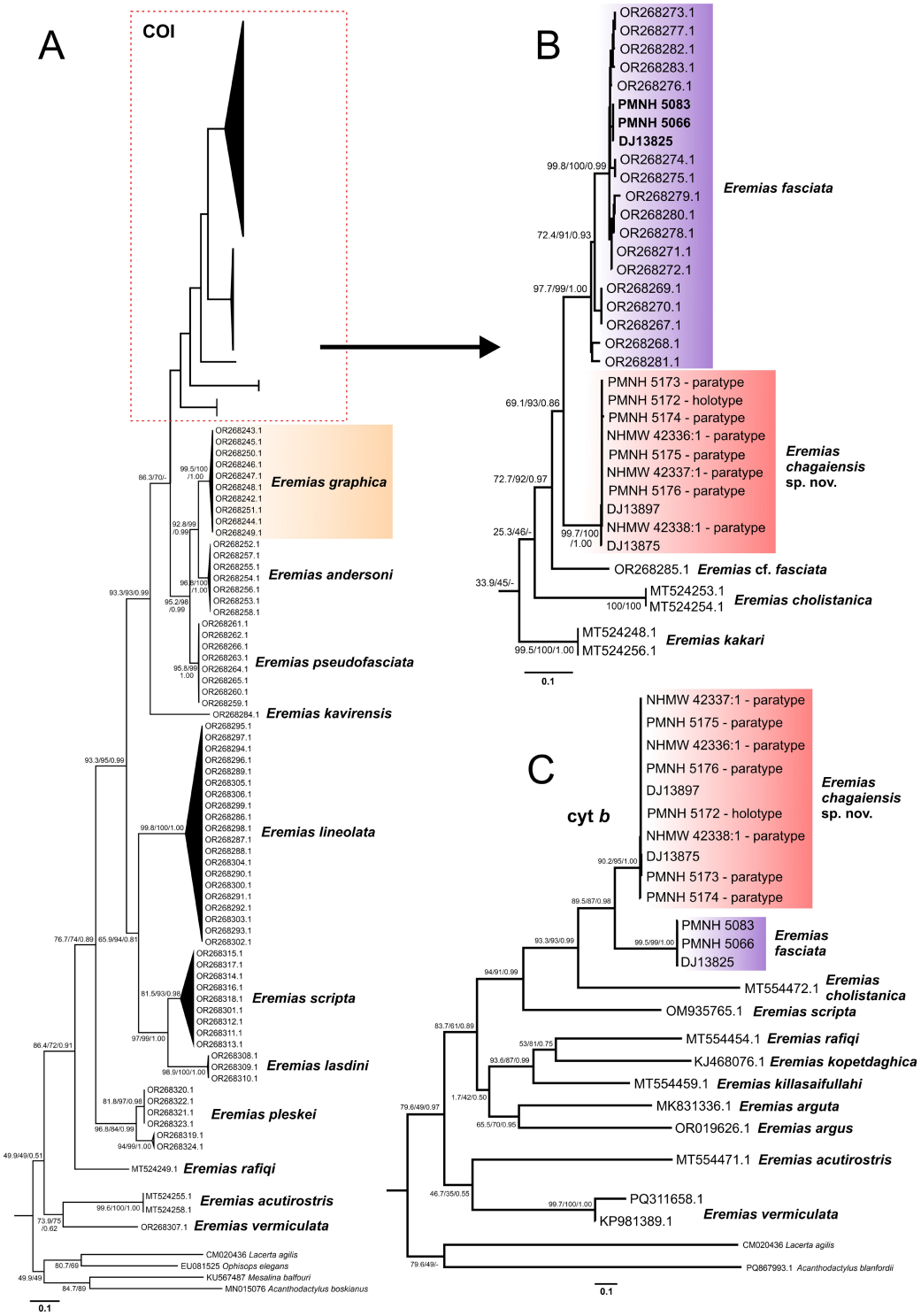



**FIGURE 1.** Maximum-likelihood phylogenetic relationships inferred from mitochondrial COI and cyt *b* sequences. **(A)** COI phylogeny of the sampled *Eremias* (*Rhabderemias*) taxa; the red dashed rectangle indicates the focal clade enlarged in panel B, and black triangles represent collapsed clades. **(B)** Enlarged section of the COI tree showing the relationships of *Eremias* (*Rhabderemias*) *chagaiensis* **sp. nov.** and *E.* (*Rhabderemias*) *fasciata*. **(C)** Cyt *b* phylogeny showing the relationship of *E. chagaiensis* **sp. nov.** to *E. fasciata* and selected congeners. Trees shown represent the maximum-likelihood topologies; Bayesian posterior probabilities were mapped onto corresponding nodes. Nodal support values are given as SH-aLRT/UFBoot/Bayesian posterior probability (PP). A dash indicates that the corresponding clade was not recovered in the Bayesian analysis. Newly generated sequences are identified by field or voucher numbers, whereas comparative sequences are labelled with their GenBank accession numbers. Type status is indicated for the holotype and paratypes of *E. chagaiensis* **sp. nov**. Branch lengths are proportional to the number of substitutions per site; scale bars are shown in each panel.

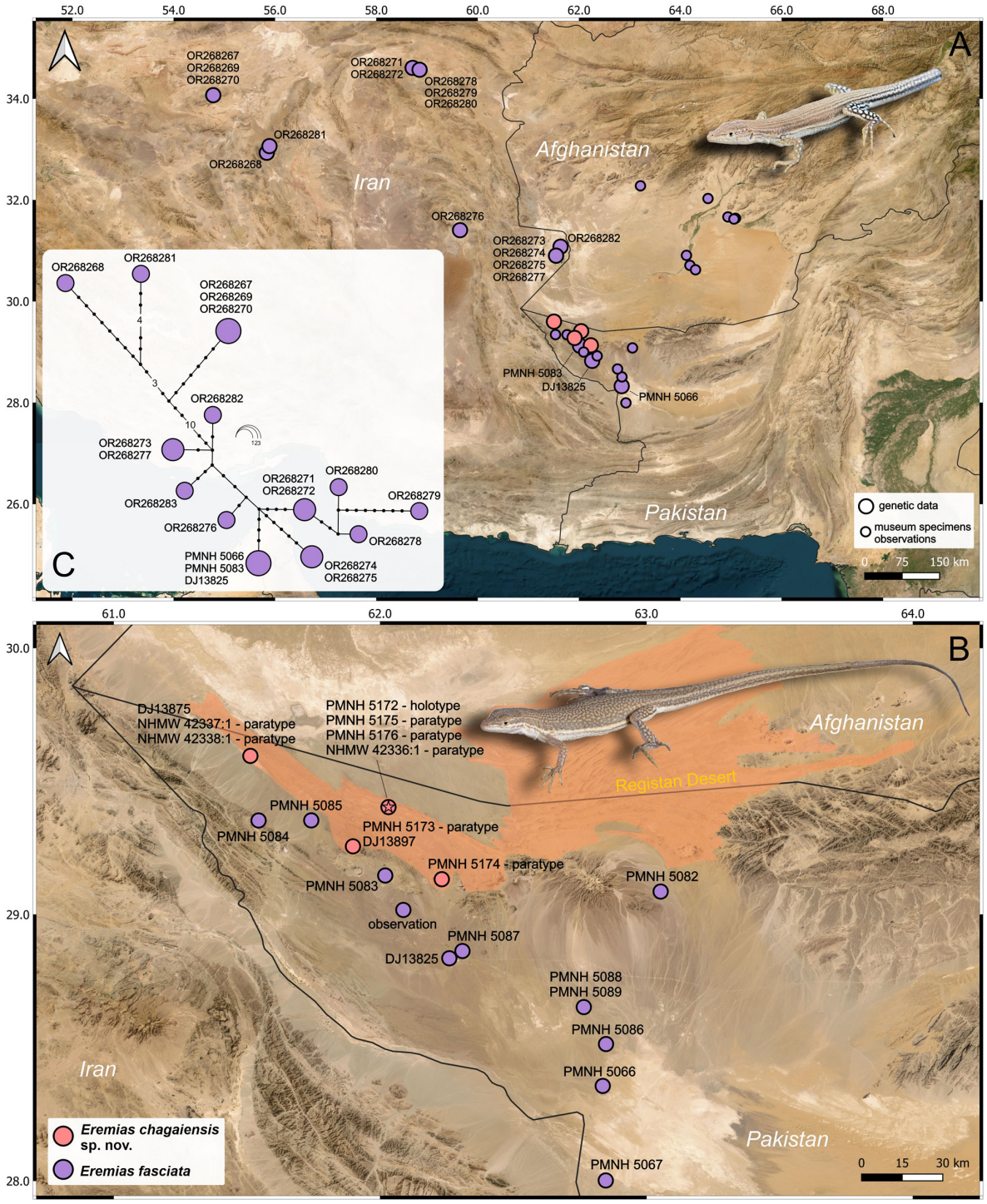



**FIGURE 2.** Geographic distribution of *Eremias* (*Rhabderemias*) *fasciata* and *E.* (*Rhabderemias*) *chagaiensis* **sp. nov. (A)** Regional distribution of *E. fasciata* across Iran, Afghanistan, and Pakistan, including newly generated and previously published genetic records and additional museum or observational records (Wagner *et al*. 2016; Jablonski & Masroor 2021; Orlova *et al*. 2023). Purple symbols represent *E. fasciata*, whereas red symbols indicate *E. chagaiensis* **sp. nov.**; symbol size denotes records with genetic data or museum/observational records, as indicated in the legend. **(B)** Detailed distribution of the two species in Pakistan. Voucher numbers and type status are indicated for the examined specimens; the holotype locality of *E. chagaiensis* **sp. nov.** is marked by a star. The orange polygon indicates the approximate extent of the Registan Desert. Photographs show representative individuals of *E. fasciata* (A) and *E. chagaiensis* **sp. nov.** (B). **(C)** TCS haplotype network based on COI sequences of *E. fasciata* across Pakistan and Iran. Node sizes are proportional to haplotype frequencies, and specimens or GenBank accession numbers sharing the same haplotype are listed adjacent to the corresponding node. Small black circles represent single mutational steps, whereas numbers along connections indicate compressed series of mutational steps.

## Systematics

### Family Lacertidae Oppel, 1811

### Genus *Eremias* Fitzinger, 1834

### Subgenus *Rhabderemias* Lantz, 1928

*Eremias chagaiensis* **sp. nov.**
(Tables 1 & Appendix 2, Figs. 1–7 & 9)
Suggested vernacular name: Chagai Racerunner
Balochi name: چاغی سوسوما ر (Chaghai Sosomaar)
Urdu name: چاغی کی تیز دوڑنے والی چپکلی (Chaghai ki tez daurhne wali chipkali)

### Holotype

PMNH 5172 (COI: PZ987611; cyt *b*: QB002738; Rag-1: QB002366), an adult male, collected from Taghazi, Nokkundi, Chagai district, Balochistan (29.4040º N, 62.0317º E; Fig. 5), elevation 833 m a. s. l., May 13, 2025, collected by R. Masroor, D. Jablonski.

### Paratypes

**Male:** PMNH 5176 (COI: PZ987608; cyt *b*: QB002735; Rag-1: QB002369). **Females:** PMNH 5173 (COI: PZ987606; cyt *b*: QB002733), PMNH 5175 (COI: PZ987610; cyt *b*: QB002737; Rag-1: QB002367), NHMW-Zoo-HS-42336:1 (COI: PZ987609; cyt *b*: QB002736), NHMW-Zoo-HS-42337:1 (COI: PZ987604; cyt *b*: QB002731; Rag-1: QB002368), NHMW-Zoo-HS-42338:1 (COI: PZ987605; cyt *b*: QB002732; Rag-1: QB002371). **Juvenile:** PMNH 5174 (COI: PZ987601; cyt *b*: QB002729; Rag-1: QB002365). Collected by R. Masroor, D. Jablonski.

PMNH 5175–76 and NHMW-Zoo-HS-42336:1 collected in Taghazi, Nokkundi, Chagai district, Balochistan on 12 (PMNH 5176, NHMW-Zoo-HS-42336:1) and 13 May 2025 (PMNH 5172, 5175) by R. Masroor, D. Jablonski; PMNH 5173 collected from Reko Diq, 29.2562º N, 61.8969º E, 908 m elevation, May 09, 2025, by R. Masroor, D. Jablonski; PMNH 5174 collected from Humai, 29.1318º N, 62.2322º E, 961 m elevation, May 01, 2025, by R. Masroor, D. Jablonski; NHMW-Zoo-HS-42337:1 and NHMW-Zoo-HS-42338:1 collected from Bagheecha, 29.5977º N, 61.5129º E, 543 m elevation, May 08, 2025, by R. Masroor, D. Jablonski (Figs. 6–7, 9).

*Eremias chagaiensis* **sp. nov.** is a member of the subgenus *Rhabderemias* based on genetic as well as morphological data. This placement follows the criterion established by Lantz (1928: 37), namely the presence of a subocular scale in direct contact with the margin of the mouth. Lantz (1928) further noted that members of the subgenus *Rhabderemias* typically retain a striped dorsal pattern from juvenile stages into adulthood. However, adult individuals of *E. graphica* as well as the presently studied *E. chagaiensis* **sp. nov.** reveal a vermiculated (finely reticulated or wavy) dorsal pattern in adults. Although *E. scripta* of the subgenus *Rhabderemias* also exhibits some dorsal vermiculation in adults, this vermiculate pattern deviates from the classical characterization of the subgenus as proposed by Lantz (1928). The persistence of a vermiculated pattern in both juveniles and adults suggests that dorsal pattern variation within *Rhabderemias* may be greater than previously recognized. Consequently, this character state should be incorporated into an updated and expanded diagnosis of the subgenus *Rhabderemias*, reflecting a broader spectrum of dorsal pattern variation than historically acknowledged.

### Morphological diagnosis

A medium-sized lacertid lizard, maximum snout-vent length (SVL) = 57.0 mm, tail 2.11–2.68 times as long as SVL (TL/SVL = 2.11–2.68), hindlimbs relatively long (HLL/SVL ratio 0.64–0.74); subocular scale reaching to

the edge of the mouth, 6–9 supralabials anterior to the subocular (mainly 6–7, rarely 9); dorsals 68–80; ventrals in 12–14 oblique longitudinal series; frontal separated from supraoculars; 10–15 femoral pores on each side, separated medially by 2–4 scales (mainly 3–4, rarely 2), the space between the femoral pores less than one-third the length of each row; fifth inframaxilare/chin shield in contact with infralabial plates of their sides; toes without fringe, encircled by four scales in a single series of 27–31 unicarinate scales underneath; tip of the fourth toe reaches to the forelimb and extends to just behind the collar.

The dorsal ground coloration of adults is predominantly beige, forming the base upon which an intricate network of light- and dark-brown vermiculations is distributed across the body dorsum. A conspicuous, broad, dark longitudinal band originates posterior to the orbit and extends posteriorly along the lateral margin of the body to the base of the tail, continuing onto the tail itself. This lateral band is well-defined and contains a series of small, contrasting white spots within it, which enhance its visual prominence. The dorsal surfaces of the limbs are dark brown and ornamented with rounded, light to yellowish spots, which may vary slightly in size and intensity among individuals. The tail tip is pale grey, contrasting with the darker proximal tail. Juveniles have approximately the same coloration and pattern as adults, but with slightly larger vermiculations and a more strongly contrasting lateral longitudinal stripe.

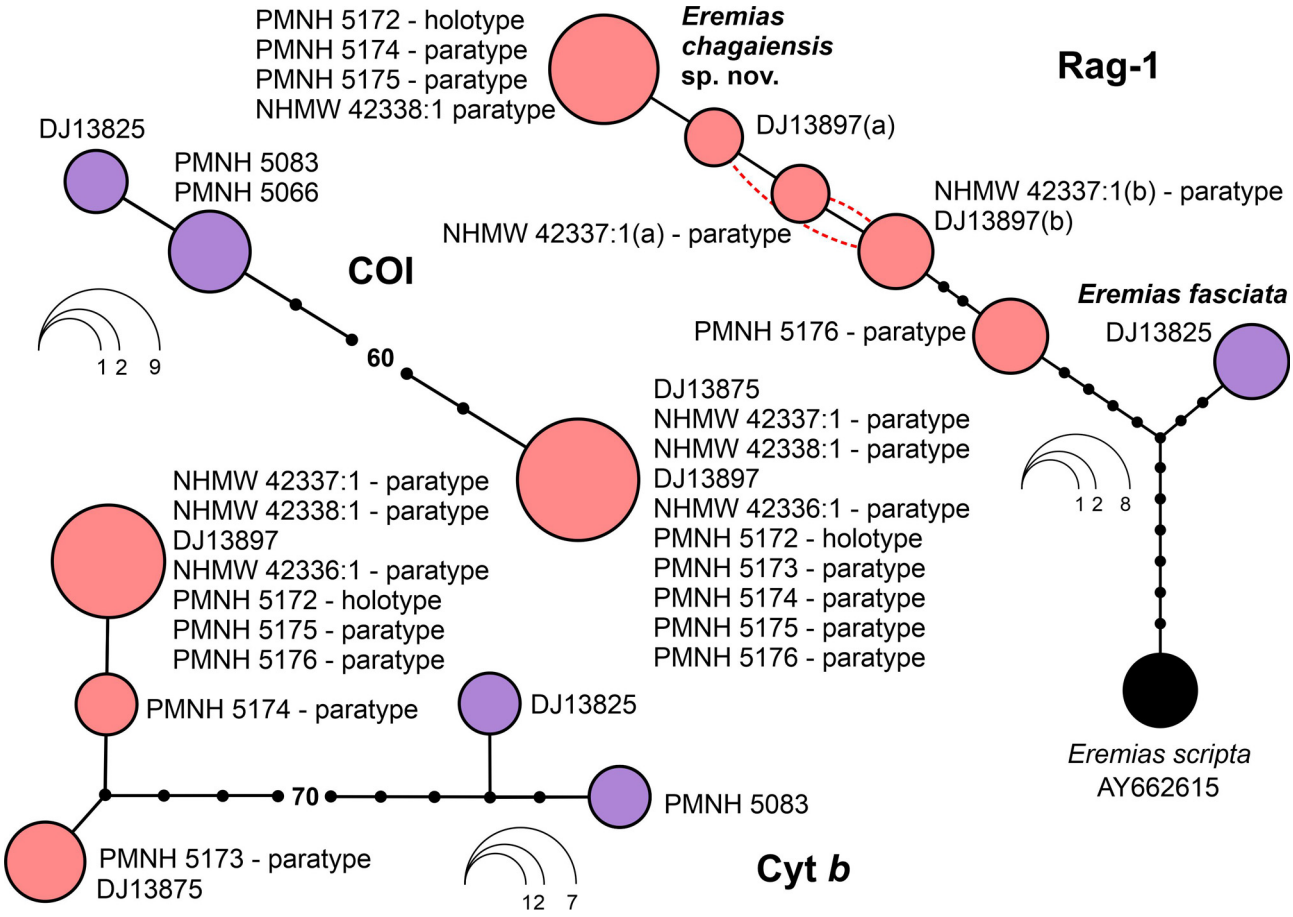



**FIGURE 3.** Haplotype networks based on mitochondrial COI and cyt *b* sequences and phased nuclear Rag-1 alleles of *Eremias* (*Rhabderemias*) *chagaiensis* **sp. nov.** and *E.* (*Rhabderemias*) *fasciata*. Red circles represent *E. chagaiensis* **sp. nov.**, purple represent *E. fasciata*, and the black circle represents the GenBank sequence of *E. scripta* used for comparison in the Rag-1 network. Node areas are proportional to haplotype frequencies, as indicated by the inset scales, and specimens sharing an identical haplotype are listed next to the corresponding node. Small black circles along connections indicate mutational steps; numbers associated with compressed long branches indicate the total number of mutational steps. For Rag-1, suffixes "a" and "b" denote the two phased alleles of heterozygous individuals, and red dashed lines connect alleles recovered from the same individual. Voucher numbers and type status are indicated and correspond to those in Figure 1.

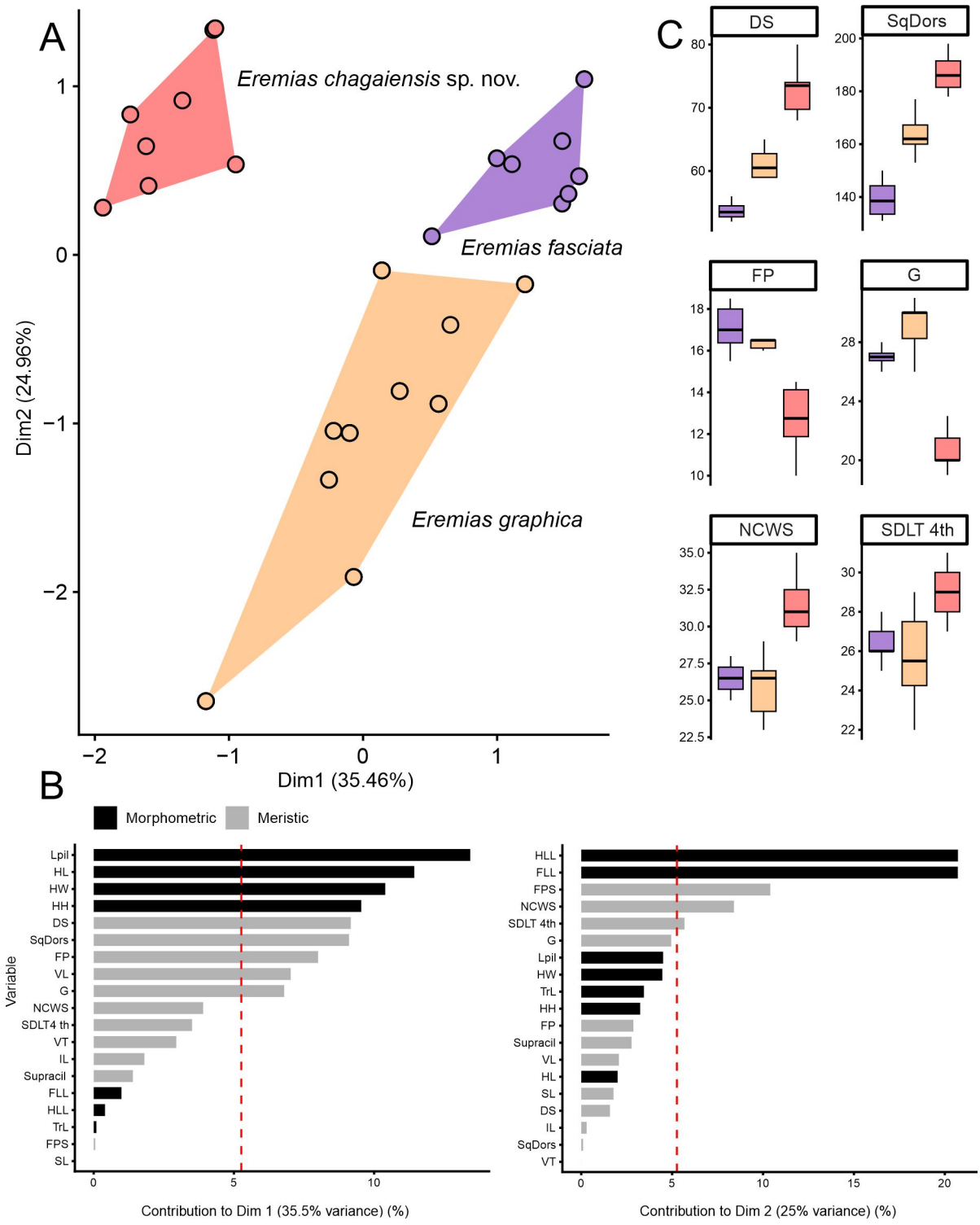



**FIGURE 4.** Multivariate morphological differentiation among *Eremias* (*Rhabderemias*) *chagaiensis* **sp. nov.**, *E.* (*Rhabderemias*) *fasciata*, and *E.* (*Rhabderemias*) *graphica*. (A) Multiple Factor Analysis (MFA) ordination of 26 specimens based on size-corrected morphometric variables and meristic characters; the first two dimensions explain 35.46% and 24.96% of the total variation, respectively. Polygons delimit the convex hulls of each taxon. (B) Contributions of individual morphometric and meristic variables to MFA Dim1 and Dim2; the dashed red line indicates the average expected contribution of a variable. (C) Boxplots of meristic characters contributing substantially to the main MFA dimensions and showing clear interspecific variation. Colors correspond to taxa as in panel A.

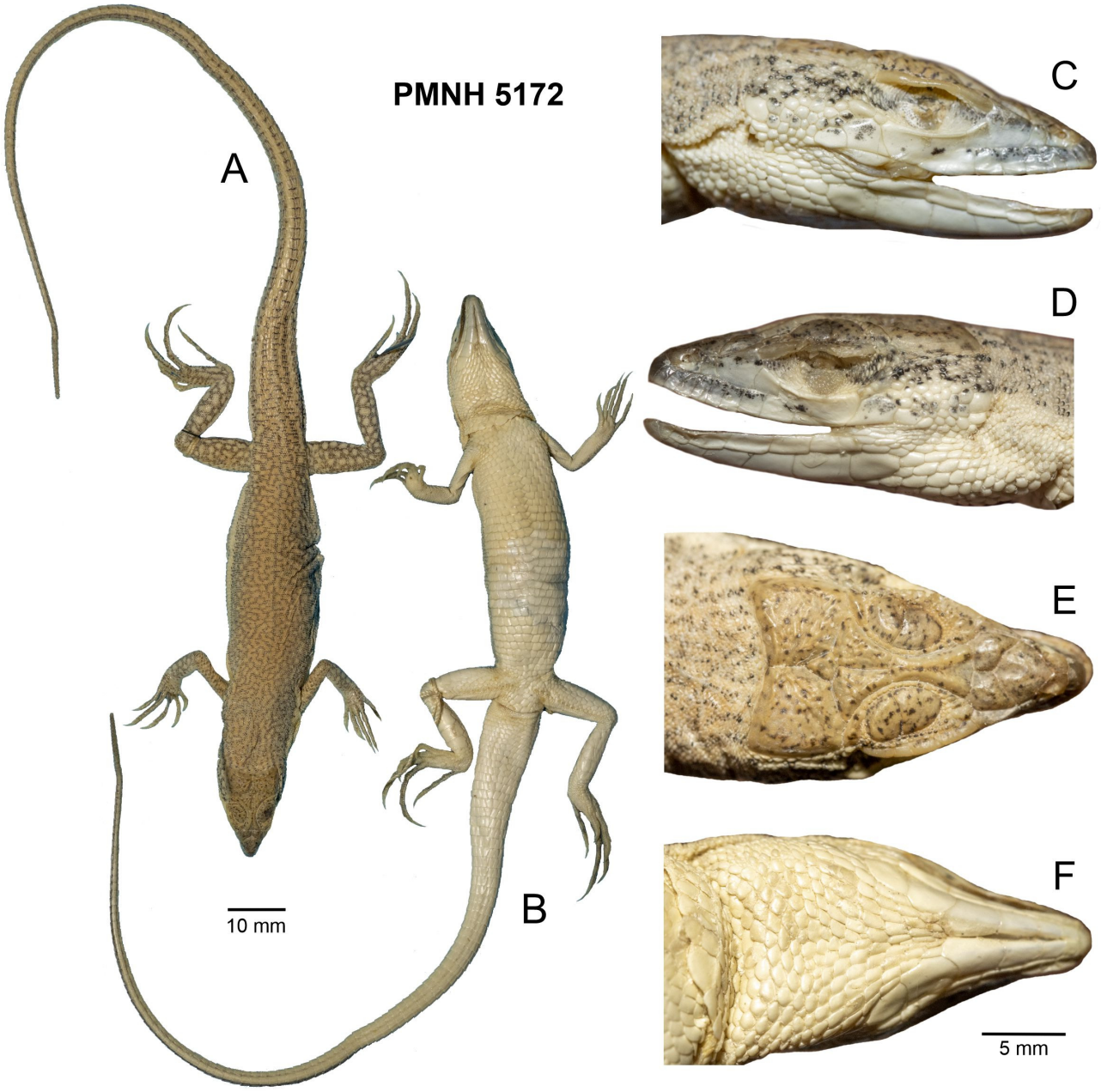



**FIGURE 5.** Holotype of *Eremias* (*Rhabderemias*) *chagaiensis* **sp. nov.** (PMNH 5172) from Taghazi, Nokkundi, Chagai District, Balochistan, Pakistan.

## Description of holotype

SVL:55.8, TL:129.2, HL:13.0, HW:8.2, HH:6.3, TrL:28.2, HLL:36.8, FLL:21.3, FrL:3.4, FrW:1.8. An adult male of *E. chagaiensis* **sp. nov.** preserved in ethanol (Fig. 5); head and body moderately depressed; tail approximately 2.3 times as long as SVL, cylindrical and depressed at the base. Head relatively long (HL/SVL ratio 0.23), ca. 1.6 times longer than wide (HW/HL ratio 0.63), head height less than head width (HH/HW, 0.77). Limbs strong, hindlimbs ca. 1.73 times as long as forelimbs (HLL/FLL = 1.73), hindlimb length corresponds to ca. 0.66 of SVL (HLL/SVL = 0.66).

Head broader than the neck; nasals, frontonasal, prefrontals, frontal, frontoparietals, interparietal and parietals are smooth and convex (Fig. 5E). Nasals are moderately swollen, three nasals, the lower in contact with the first three supralabials on the right and left side, its contact with the rostral lacking (Fig. 5C–D). Supranasals in contact with rostral and first supralabial, the supranasal suture is about one-fourth of the length of frontonasal, whose

breadth in turn is ca. 1.13 times its length; length of prefrontals 1.4 times its width, joined by a median suture whose length is greater than the supranasal suture; frontal slightly less than two times as long as broad (FrL/FrW = 1.9), its length slightly less than its distance from the tip of the snout, narrow behind; parietals smooth, their length approximately equal to their width; interparietal smooth, more than half of the length of frontoparietals; no occipital. Two large supraoculars, the anterior one slightly larger than posterior, the space anterior to supraoculars filled by few small and three to five larger granules; both supraoculars separated from the frontal of their sides by a single row of granules while separated from the supraciliaries by a series of two rows of small granules (Fig. 5E), behind the two large supraoculars a single, comparatively medium-sized, granule exists; four supraciliaries on both sides, the most anterior longest, its length shorter than its distance from the first loreal. Rostral pentagonal, broader than high, narrower beneath than above; anterior loreal slightly higher than wide, shorter than the second loreal which is longer than high; supralabials nine on the right side, eleven on the left side; subocular bordering the mouth, wedged between seventh and eighth supralabials on the right side whereas ninth and tenth on the left side (Fig. 5C–D). Temporals smooth, a large scale above ear; auricular denticulation minute, three to four small scales forming slight denticulation anteriorly. Lower eyelid covered with numerous small semi-transparent scales.

Six infralabials on each side, gradually increasing in size posteriorly. Five pairs of chin shields; anterior three completely in contact, the fourth one separated by six gulars, the fifth one is in contact with sixth infralabial of their sides. Collar curved, free, serrated and composed of seven plates larger than adjacent gulars, the median one slightly larger than the others. Gular fold distinct, 20 gular scales in a straight line between the symphysis of the chin shields and the collar (Fig. 5F).

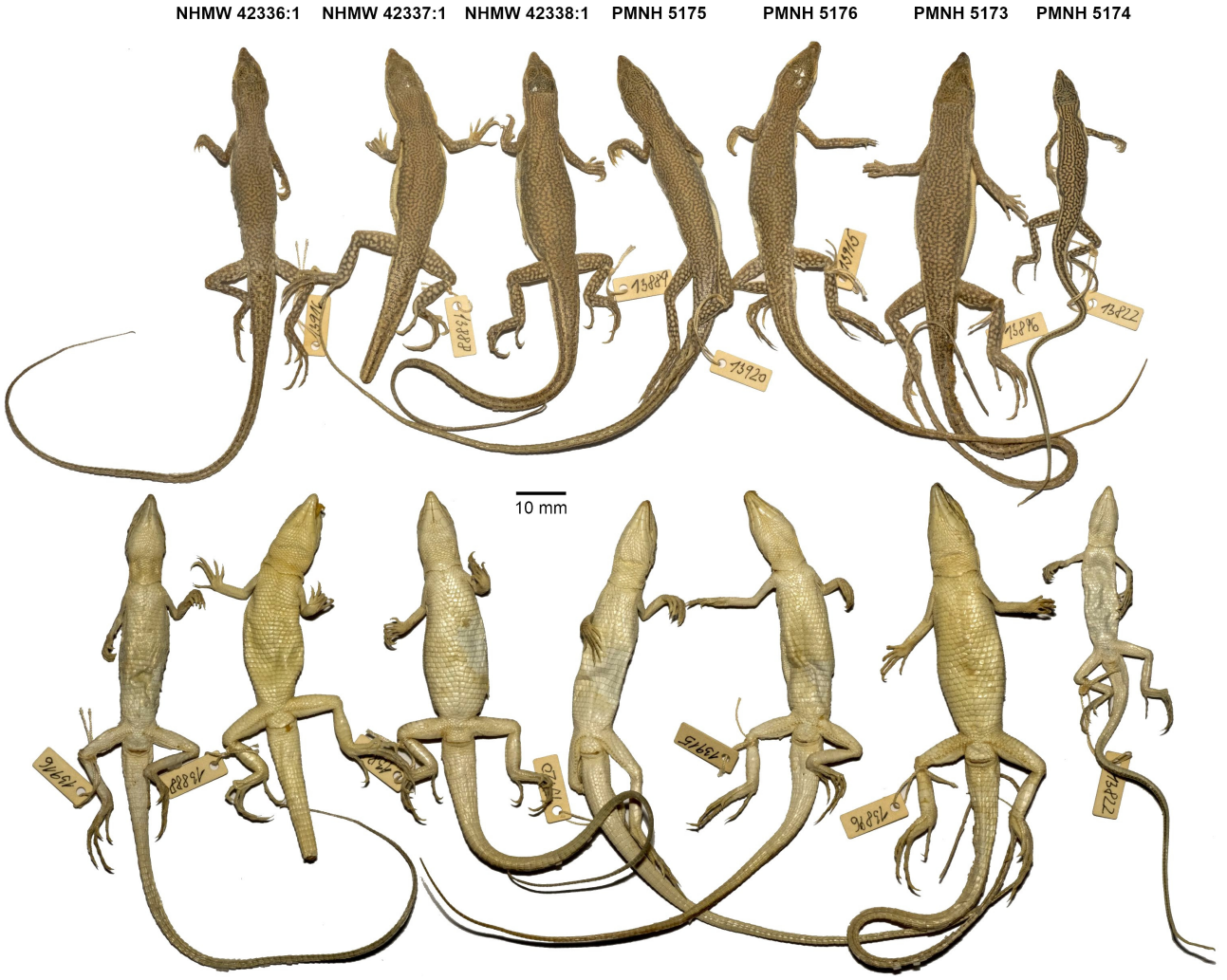



**FIGURE 6.** Dorsal and ventral views of paratypes of *Eremias* (*Rhabderemias*) *chagaiensis* **sp. nov.**, representing different ontogenetic stages and originating from several localities in northwestern Balochistan, Pakistan. Photographs by Daniel Jablonski.

Dorsal scales granular, smooth, 74 across the middle of the body. Ventral plates broader than long (except for outermost series), forming oblique longitudinal series of 14 plates across mid-belly and 35 transverse rows counted from behind collar to vent; first few rows of ventral scales in the pectoral region behind collar longer than broad, the first row is twice as long as broad. Precloacal region with nine enlarged median plates just above the vent.

The forelimb is approximately 1.6 times as long as the head, upper surface of the arm with rhombic, smooth scales. Scales on the upper surface of hindlimbs similar to dorsals, varying in size; ventral surface of hindlimbs covered by enlarged plates, the lower surface of the tibia with one row of comparatively larger plates, the tip of the fourth toe reaches to the forelimb and extends to just behind the collar; 10 femoral pores under each side of thigh, the two series separated by four scales, length of the interfemoral space about one-third length of each row. Toes slender, compressed, with no fringe. Subdigital lamellae unicarinate, in a single row of 27 scales under the 4th toe, a total of four scales around the 4$^{th}$ toe. Upper caudal scales oblique, truncate, strongly and diagonally keeled, 34 scales in the 9$^{th}$–10$^{th}$ annulus behind the postcloacal granules.

## Coloration in life

The dorsal ground coloration of adults (Fig. 5A) is predominantly beige, forming the base upon which the characteristic pattern is superimposed. The dorsal pattern consists of an intricate network of light and dark brown vermiculated, irregular lines distributed across the body dorsum. These vermiculations create a marbled appearance and do not organize into distinct or continuous longitudinal dark stripes along the dorsum. A conspicuous, broad, dark longitudinal band originates posterior to the orbit and extends posteriorly along the lateral margin of the body to the base of the tail, continuing onto the tail itself. This lateral band is well-defined and contains a series of small, contrasting white spots within it, which enhance its visual prominence. Below this primary lateral band, a narrower and less contrasting dark longitudinal stripe arises from behind the posterior upper labials and extends along the flanks, although it may be faint or partially obscured in some individuals. The dorsal surfaces of the limbs are dark brown and ornamented with rounded, light to yellowish spots, which may vary slightly in size and intensity among individuals. These spots contribute to the overall vermiculated and mottled appearance of the species. The ventral surfaces are uniformly whitish, lacking conspicuous markings or pigmentation (Fig. 5B). The distal portion (tip) of the tail exhibits a lighter greyish hue compared to the proximal dorsal coloration, producing a subtle but distinct tonal transition toward the tail extremity. Juveniles show a similar coloration and pattern to adults but have slightly larger vermiculations and a more contrasting lateral longitudinal stripe (Figs. 7B, 9).

## Variations in paratypes

Paratypes of *E. chagaiensis* **sp. nov.** agree with the description of the holotype with some differences given in Table 1 and Figs. 6 & 9. Apart from sex, the specimens differ in the arrangement of supralabials i.e., subocular wedged between 6$^{th}$ and 7$^{th}$ supralabials on the right side and 7$^{th}$ and 8$^{th}$ on the left side in NHMW-Zoo-HS-42336:1 and PMNH 5174; 7$^{th}$ and 8$^{th}$ supralabials on both sides in PMNH 5175 and 5176; 6$^{th}$ and 7$^{th}$ on both sides in NHMW-Zoo-HS-42337:1; 7$^{th}$ and 8$^{th}$ on the right and 6$^{th}$ and 7$^{th}$ on the left in NHMW-Zoo-HS-42338:1. The arrangement of postmentals has a similar pattern in the paratypes. In all specimens of the type series including the holotype, the fifth chin shield is in contact with the infralabials. The counts of dorsal, ventral, gular, collar and caudal scales at the 9th–10th whorls, as well as subdigital lamellae beneath the fourth toe, vary among specimens within the ranges given in Table 1. The infranasal is not in contact with the rostral in all type specimens including the holotype.

## Comparison

*Eremias chagaiensis* **sp. nov.** is distinguishable from the other compared species of the subgenus *Rhabderemias* (*E. andersoni* Darevsky & Szczerbak, 1978; *E. cholistanica* Baig & Masroor, 2006; *E. fasciata* Blanford, 1874; *E. kakari* Masroor *et al*., 2020; *E. lineolata* (Nikolsky, 1897); *E. pleskei* Nikolsky, 1905; *E. pseudofasciata* Orlova *et al*., 2023; *E. scripta* (Strauch, 1867); *E. vermiculata* Blanford, 1875) by vermiculated dorsal body pattern on the adults (vs. striped pattern in all other species except *E. vermiculata* and the recently described *E. graphica* Orlova *et al*., 2023).




**FIGURE 7.** Live individuals and habitats of *Eremias* (*Rhabderemias*) *chagaiensis* **sp. nov.** from Chagai District, Balochistan, Pakistan. (A) An adult female from Bagheecha; (B) live juvenile paratype (PMNH 5174) from Humai (1 May 2025); (C) close-up view of the type locality at Taghazi (11 May 2025); (D) overview of the type locality from a high sand dune, near the border with Afghanistan (11 May 2025); (E) habitat of the new species at Humai (1 May 2025); (F) habitat of the new species at Bagheecha, approximately 5 km from the border with Afghanistan (6 May 2025), the gravelly areas represent habitat typical of *E. fasciata*, whereas the low sand dunes are characteristic of the new species. Photographs by Daniel Jablonski.

*Eremias chagaiensis* **sp. nov.** can be distinguished from its regionally co-occurring species *E. fasciata* by the following characters: vermiculate dorsal pattern versus striped pattern in *E. fasciata*, coloration of the tympanic region, yellow in *E. fasciata* versus white in *E. chagaiensis* **sp. nov.** *Eremias chagaiensis* **sp. nov.** has 68–80 dorsal scales around midbody as compared to *Eremias fasciata* which possesses 44–50 (Anderson 1999) or 52–56 scales (data from the Pakistani specimens of genetically and morphologically validated *E. fasciata*). The number of gular scales in *E. chagaiensis* **sp. nov.** ranges from 19–24 as compared to 21–30 in *E. fasciata*. The number of femoral pores in *Eremias chagaiensis* **sp. nov.** ranges from 10–15 on each side beneath the thigh as compared to 15–19

in *E. fasciata*. Similarly, other morphological and meristic characters differ between *E. chagaiensis* **sp. nov.** and *E. fasciata* including fewer ventral scales in longitudinal rows (VL) (12–14 versus 14–17) and ventral scales in transverse rows (VT) (32–35 versus 29–38).

Besides the dorsal color and pattern, *E. chagaiensis* **sp. nov.** differs from *E. andersoni* by a greater SVL (max SVL) of 57.0 mm versus 40.0 mm, vermiculated pattern versus longitudinal stripes on the dorsum of *E. andersoni*, more ventral scale rows (VT) in *E. chagaiensis* **sp. nov.** (32–35 versus 28–29) and greater number of dorsal scales (68–80 versus 56–58). In addition, *E. andersoni* has light-bluish coloration at the tip of the tail, whereas *E. chagaiensis* **sp. nov.** has a light-greyish tail tip.

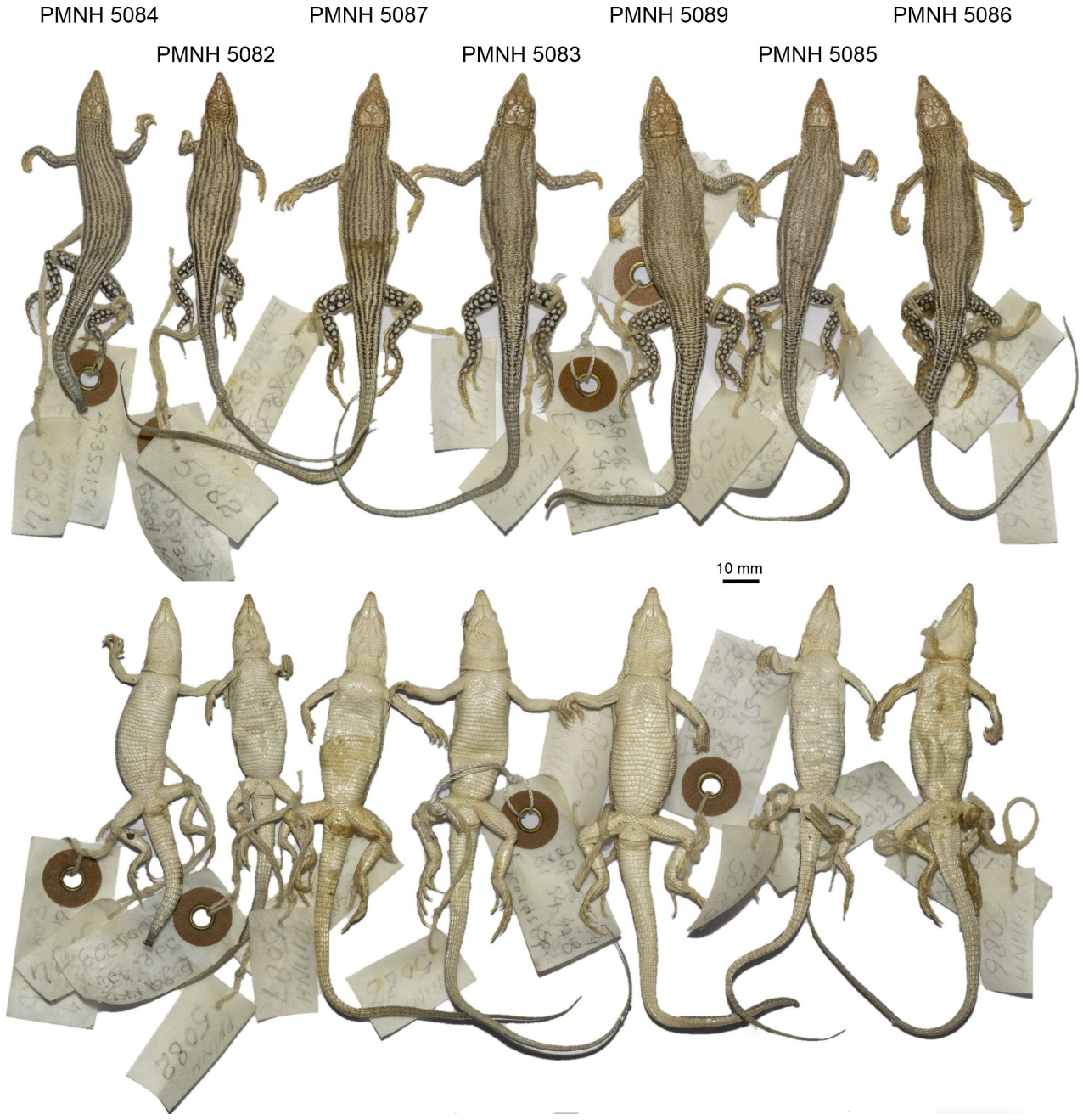



**FIGURE 8.** Dorsal and ventral colour patterns of adult specimens of *Eremias* (*Rhabderemias*) *fasciata* from different localities in the Nokkundi region, Chagai District, Balochistan, Pakistan. Photographs by Daniel Jablonski.

Although *E. chagaiensis* **sp. nov.** and *E. graphica* share a vermiculate dorsal pattern, they differ in several meristic characters with non-overlapping ranges: dorsal scales around midbody (68–80 versus 59–65; although 54–65 is reported in the diagnosis of *E. graphica* by Orlova *et al.* 2023: p. 362), gular scales (19–24 versus 26–31),

and the total number of femoral pores on both thighs (20–29 versus 31–36). Additional differences, although with partially overlapping ranges, include the tail-length-to-SVL ratio (2.11–2.68 versus 1.69–2.36), scales around the ninth and tenth caudal whorls (29–35 versus 23–29), longitudinal rows of ventral scales (12–14 versus 14–18), and subdigital lamellae under the fourth toe (27–31 versus 22–29). The coloration and pattern of juveniles of E. graphica have not been described, precluding direct comparison with juveniles of *E. chagaiensis* **sp. nov.**

Apart from its distribution in western Balochistan, Pakistan, *E. chagaiensis* **sp. nov.** differs from *E. lineolata* by the vermiculated dorsal pattern versus longitudinal dark stripes in *E. lineolata* and the number of scales around the 9th and 10th tail segment (NCWS) of 29–35 versus 12–17 in *E. lineolata*. Besides, *E. chagaiensis* **sp. nov.** has 68–80 dorsal scales on the midbody as compared to 54–62 in *E. lineolata*.

*Eremias chagaiensis* **sp. nov.** can be clearly distinguished from *E. scripta* by lacking the lateral fringes on the toes (versus present), a higher number of dorsal scales with 68–80 versus 55–69 and a higher number of NCWS of 29–35 versus 17–28. Although the dorsal patterns in *E. scripta* can be vermiculated to the extent that the middle lineolate pattern transforms into vermiculation (versus pattern of vermiculation on the whole body of *E. chagaiensis* **sp. nov.**), the new species clearly differs on the basis of other morphological characters.

*Eremias chagaiensis* **sp. nov.** differs from *E. cholistanica* by vermiculate dorsal pattern versus striped patterns in *E. cholistanica* and higher number of dorsal scales (68–80 versus 51–63).

*Eremias chagaiensis* **sp. nov.** differs from *E. pseudofasciata* by vermiculate dorsal pattern versus striped patterns in the latter species, and by a combination of characters including higher number of dorsal scales (68–80 versus 44–51), fewer femoral pores (10–15 versus 14–19), gulars (19–24 versus 26–33) and VL (12–14 versus 13–16).

Multivariate analysis of morphometric and meristic characters further supported the morphological differentiation of the new species from the phylogenetically and/or morphologically closely related lineages *E. fasciata* and *E. graphica* (Fig. 4).

## Etymology

The name of the new species is derived from Chagai (Balochi: چاغی ; also spelled Chaghai), a city, district, and desert in western Balochistan Province, Pakistan. The species is currently known only from this region, and the name highlights the importance of Chagai for biodiversity research and conservation.

## Distribution

*Eremias chagaiensis* **sp. nov.** is currently known from four localities: Taghazi, Humai, Reko Diq, and Bagheecha in western Chagai District, Balochistan Province, Pakistan, close to the border with Afghanistan. All known records are situated within the Registan-North Pakistan sandy desert ecoregion, which belongs to the Deserts and Xeric Shrublands biome of the Palearctic realm (Olson *et al.* 2001). Based on the available occurrence records, the estimated extent of occurrence (EOO) of the new species is approximately 911 km², whereas the area of occupancy (AOO), calculated using a 2 × 2 km grid, is 16 km², both relevant for IUCN Red List assessments. The known distribution lies within the eastern part of the Iranian Plateau and represents the southeastern continuation of the broader Registan desert system. Similar sandy and gravelly habitats extend westward across the international border into southwestern Afghanistan, particularly toward the southern parts of Helmand and Kandahar provinces and to eastern Iran. The occurrence of the species in this adjoining region is therefore plausible, although it remains unconfirmed. Additional surveys are required to determine its actual distributional limits in Afghanistan, Iran and other areas of Pakistan. Consequently, the available evidence is insufficient to assign the species to a threatened category under the IUCN Red List Categories and Criteria solely on the basis of its documented range.

## Habitat and natural history

The type locality is situated in a hyper-arid desert landscape composed of low, active or weakly stabilized sand dunes and sand sheets embedded within an extensive matrix of gravel plains, deflation surfaces, and isolated rocky outcrops (Fig. 7C–F). Although gravelly and rocky substrates dominate parts of the surrounding landscape, *E. chagaiensis*

**sp. nov.** was observed exclusively in sandy habitats. On the other hand, its sister species *E. fasciata* is present in the area on gravel plains and around sand dunes. Vegetation cover within these habitats is sparse and discontinuous and consists primarily of scattered xerophytic and halophytic shrubs, including *Haloxylon salicornicum*, *Calligonum polygonoides*, and species of *Zygophyllum*.

Individuals were encountered on loose sand, particularly on low dunes, sand sheets, and wind-deposited sandy patches occurring between or adjacent to gravel plains and rocky formations. The species was not observed on exposed gravel or rocky substrates. Within the sandy habitat, individuals were frequently recorded near the bases of shrubs, which provide structural cover and refuge from predators and extreme surface temperatures. Burrows were typically excavated beneath or adjacent to shrub root systems, where the sand was relatively stabilized. Shrub patches may also represent areas of locally increased arthropod abundance and therefore suitable foraging sites.

During the survey period, surface activity of the new species was concentrated in two daily intervals, approximately between 09:00 and 12:00 h and between 15:00 and 18:00 h. Individuals were rarely observed during the hottest part of the day, when they retreated beneath shrubs or into burrows. This bimodal activity pattern is consistent with behavioural thermoregulation under hyper-arid desert conditions.

Several reptile species were recorded in the broader habitat mosaic surrounding the type locality, including *Bunopus tuberculatus* Blanford, 1874, *Phrynocephalus euptilopus* Alcock & Finn, 1897, *P. maculatus* Anderson, 1872, *Rhinogekko* sp., *Teratoscincus keyserlingii* Strauch, 1863, and *Eremias fasciata* Blanford, 1874. However, these taxa were not necessarily restricted to the same sandy microhabitats occupied by *E. chagaiensis* **sp. nov.**

**Conservation status.** *Eremias chagaiensis* **sp. nov.** is currently known from four closely situated localities in western Chagai District, indicating a highly restricted documented distribution. However, the presently known records probably represent a minimum estimate of its range, as potentially suitable sandy habitats extend northwards into the poorly surveyed Registan Desert of Afghanistan. Furthermore, no continuing decline in the extent or quality of its habitat, severe fragmentation, extreme fluctuations, or clearly defined threat-based locations can currently be demonstrated. Consequently, the available evidence is insufficient to assign the species to a threatened category under IUCN solely on the basis of its documented range. We therefore recommend that *E. chagaiensis* **sp. nov.** be provisionally classified as "Data Deficient" pending targeted surveys and an assessment of threats to its dune habitats in western Chagai and adjacent Afghanistan.

### Confirmation of *Eremias fasciata* for Pakistan

Figs. 1-4, 8, 9

### Material examined

**Pakistan: Balochistan Province:** PMNH 5066, Nokkundi region, 28 September 2022, 28.3555° N, 62.8363° E, 503 m elevation, collected by R. Masroor (excluded from morphological analyses due to poor post-fixation condition); PMNH 5067, 28 September 2022, 28.0210° N, 62.8799° E, 499 m elevation, collected by R. Masroor (not included in morphological analyses); PMNH 5082, Nokkundi region, 3 May 2023, 29.0869° N, 63.0536° E, 875 m elevation, collected by R. Masroor; PMNH 5083, Nokkundi region, 30 April 2023, 29.1483° N, 62.0205° E, 996 m elevation, collected by R. Masroor; PMNH 5084, western part of the Nokkundi region, 28 April 2023, 29.3531° N, 61.5442° E, 932 m elevation, collected by R. Masroor; PMNH 5085, 7 May 2023, Nokkundi region, 29.3531°N, 61.7406°E, 668 m elevation; PMNH 5086, Nokkundi region, 7 May 2023, 28.5129° N, 62.8485° E, 527 m elevation, collected by R. Masroor; PMNH 5087, Nokkundi region, 7 May 2023, 28.8347°N, 62.3115°E, 728 m elevation, collected by R. Masroor (Fig. 8); PMNH 5088 and PMNH 5089, Nokkundi region, 8 May 2023, 28.6572° N, 62.7613° E, 622 m elevation, collected by R. Masroor; DJ13825 (no morphological data taken), Tozghi, 1 May 2025, 28.8380° N, 62.2622° E, 691 m elevation, collected by R. Masroor, D. Jablonski.

An additional individual was observed at Ware Sahib Chah, 30 April 2025, 29.0182°N, 62.0882°E, 858 m elevation, observed by D. Jablonski (Fig. 2, "observation").

Molecular data were obtained from PMNH 5083 (COI: PZ987599; cyt *b*: QB002726), PMNH 5066 (COI: PZ987600; cyt *b*: QB002727), and DJ13825 (COI: PZ987602; cyt *b*: QB002728; Rag-1: QB002372).

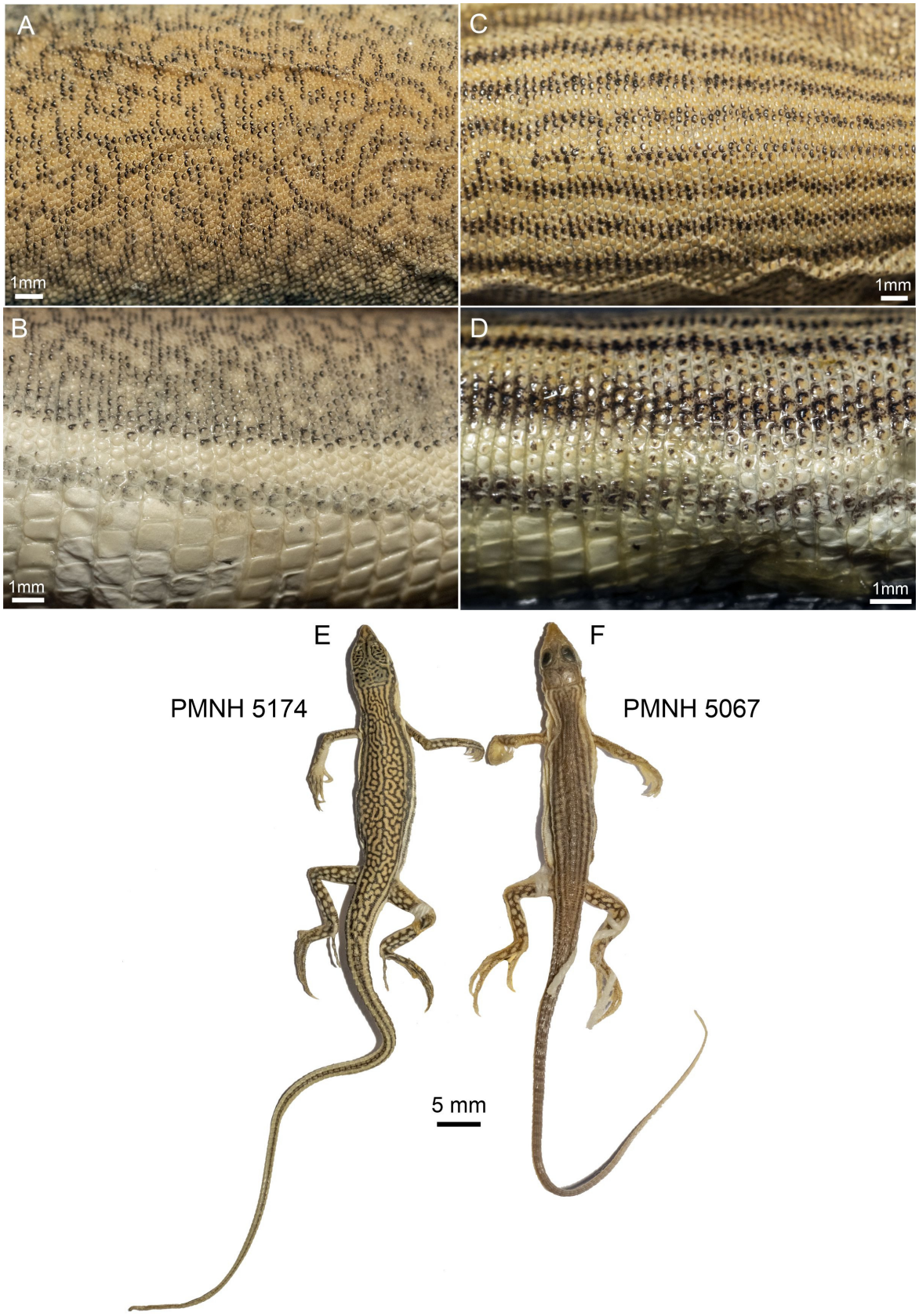



**FIGURE 9.** Colour patterns of *Eremias* (*Rhabderemias*) *chagaiensis* **sp. nov.** and *E.* (*Rhabderemias*) *fasciata*. (A, C) Dorsal patterns of adult *E. chagaiensis* **sp. nov.** and *E. fasciata*, showing vermiculate and lineolate patterns, respectively. (B, D) Lateral patterns of adult *E. chagaiensis* **sp. nov.** and *E. fasciata*, respectively; note the strongly contrasting lateral longitudinal stripe in *E. fasciata*. (E, F) Juveniles of *E. chagaiensis* **sp. nov.** and *E. fasciata*, showing vermiculate and lineolate patterns, respectively. Photographs by Daniel Jablonski.

**TABLE 1.** Morphometric and meristic data of the type series of *Eremias* (*Rhabderemias*) *chagaiensis* **sp. nov.** including ratios of important characters. For abbreviation of characters, see Material and methods (N/A = data not available, + = in contact, - = separated, rg= regenerated, br= broken, ND= not determined). All measurements are in mm.

| Voucher No. | PMNH 5172 | PMNH 5173 | PMNH 5174 | PMNH 5175 | PMNH 5176 | NHMW-Zoo-HS-42336:1 | NHMW-Zoo-HS-42337:1 | NHMW-Zoo-HS-42338:1 |
|---|---|---|---|---|---|---|---|---|
| Sex | Male | Female | ND | Female | Male | Female | Female | Female |
| Age | adult | adult | juvenile | adult | adult | adult | adult | adult |
| Types | Holotype | Paratype | Paratype | Paratype | Paratype | Paratype | Paratype | Paratype |
| **Morphometry** | | | | | | | | |
| SVL | 55.8 | 57.0 | 36.0 | 52.0 | 53.0 | 51.7 | 49.4 | 51.8 |
| TL | 129.2 | 153.0 | 76.0 | 136.4 | 109.1 (rg) | 136.8 | 26.5(br) | 116.1 (rg) |
| TL/SVL | 2.32 | 2.68 | 2.11 | 2.62 | ND | 2.65 | ND | ND |
| Lpil | 12.2 | 13.2 | 8.7 | 12.1 | 12.3 | 11.9 | 11.5 | 11.0 |
| HL | 13.0 | 13.6 | 9.2 | 13.0 | 13.1 | 12.1 | 12.2 | 12.1 |
| HW | 8.2 | 8.2 | 4.7 | 7.2 | 7.3 | 7.7 | 7.0 | 7.1 |
| HH | 6.3 | 6.2 | 3.1 | 5.2 | 4.5 | 6.2 | 5.1 | 5.2 |
| TrL | 28.2 | 28.6 | 19.1 | 26.1 | 27.5 | 24.5 | 25.5 | 27.3 |
| NL | 18.7 | 19.5 | 12.6 | 18.6 | 18.9 | 18.0 | 17.2 | 16.5 |
| FNL | 2.2 | 2.5 | 1.3 | 2.0 | 1.9 | 1.8 | 2.0 | 1.8 |
| FrL | 3.4 | 4.1 | 2.2 | 3.2 | 3.4 | 3.4 | 3.2 | 3.1 |
| PFL | 2.1 | 2.2 | 1.4 | 2.0 | 2.1 | 1.8 | 1.8 | 1.6 |
| PFW | 1.5 | 1.5 | 1.0 | 1.3 | 1.7 | 1.3 | 1.2 | 1.3 |
| FrW | 1.8 | 2.0 | 1.2 | 2.0 | 2.1 | 1.8 | 1.7 | 1.6 |
| FLL | 21.3 | 23.6 | 13.2 | 22.7 | 20.2 | 21.4 | 19.1 | 20.0 |
| HLL | 36.8 | 38.6 | 23.8 | 37.2 | 34.2 | 38.2 | 33.5 | 33.0 |
| HLL/SVL | 0.66 | 0.68 | 0.66 | 0.72 | 0.65 | 0.74 | 0.68 | 0.64 |
| HRL | 13.3 | 14.1 | 8.0 | 12.8 | 14.0 | 12.5 | 11.7 | 11.2 |
| FL | 10.6 | 11.1 | 7.7 | 10.5 | 9.3 | 10.7 | 10.9 | 10.0 |
| CL | 11.7 | 11.8 | 8.2 | 10.3 | 9.0 | 10.1 | 10.9 | 10.1 |
| LFPR | 7.2 | 10.4 | 7.1 | 8.2 | 8.7 | 9.2 | 8.9 | 7.2 |
| LFPS | 2.2 | 2.0 | 1.6 | 2.2 | 1.8 | 2.0 | 2.0 | 2.1 |
| **Meristic** | | | | | | | | |
| DS | 74 | 68 | 74 | 74 | 73 | 80 | 69 | 70 |
| G | 20 | 20 | 19 | 21 | 23 | 24 | 20 | 20 |
| Coll | 7 | 6 | 7 | 8 | 6 | 6 | 7 | 7 |
| FP (r/l) | 10/10 | 12/12 | 11/12 | 15/14 | 11/14 | 14/14 | 14/15 | 13/13 |
| FPS | 4 | 3 | 2 | 3 | 3 | 3 | 4 | 4 |
| VL | 14 | 13 | 12 | 14 | 14 | 14 | 14 | 14 |
| VT | 35 | 33 | 32 | 33 | 35 | 33 | 33 | 32 |
| NCWS | 34 | 31 | 29 | 32 | 30 | 35 | 30 | 31 |
| SDLT 4th | 27 | 28 | 28 | 30 | 31 | 29 | 29 | 30 |
| SAT 4th | 4 | 4 | 4 | 4 | 4 | 4 | 4 | 4 |
| SDLF 4th | 24 | 25 | 24 | 23 | 23 | 23 | 23 | 23 |
| SqDors | 190 | 198 | 180 | 182 | 196 | 188 | 178 | 184 |

*.....continued on the next page*

**TABLE 1.** (Continued)

| Voucher No. | PMNH 5172 | PMNH 5173 | PMNH 5174 | PMNH 5175 | PMNH 5176 | NHMW-Zoo-HS-42336:1 | NHMW-Zoo-HS-42337:1 | NHMW-Zoo-HS-42338:1 |
|---|---|---|---|---|---|---|---|---|
| Sex | Male | Female | ND | Female | Male | Female | Female | Female |
| Age | adult | adult | juvenile | adult | adult | adult | adult | adult |
| Types | Holotype | Paratype | Paratype | Paratype | Paratype | Paratype | Paratype | Paratype |
| SL (r/l) | 9/11 | 9/9 | 8/9 | 9/10 | 10/10 | 9/9 | 8/8 | 10/9 |
| SLAS (r/l) | 7/9 | 7/9 | 6/7 | 7/7 | 7/7 | 6/7 | 6/6 | 7/6 |
| IL (r/l) | 6/6 | 6/7 | 4/5 | 7/7 | 6/6 | 6/6 | 8/6 | 6/6 |
| Submax | 5 | 5 | 5 | 5 | 5 | 5 | 5 | 5 |
| Supracil (r/l) | 4/4 | 4/4 | 4/5 | 4/4 | 4/5 | 4/5 | 4/4 | 4/4 |
| **Categorical** | | | | | | | | |
| FMIL | + | + | + | + | + | + | + | + |
| SOM | + | + | + | + | + | + | + | + |
| FSO | - | - | - | - | - | - | - | - |
| INTR | - | - | - | - | - | - | - | - |
| Gran | + | + | + | + | + | + | + | + |
| LB | - | - | - | - | - | - | - | - |
| FSpots | + | + | + | + | + | + | + | + |

**TABLE 2.** Morphometric and meristic data of the *Eremias* (*Rhabderemias*) *fasciata* including ratios of important characters. For abbreviation of characters, see material and methods (N/A = data not available, + = in contact or present, - = separated or absent, rg= regenerated, br= broken, ND= not determined). All measurements are in mm.

| **Voucher No.** | PMNH 5082 | PMNH 5083 | PMNH 5084 | PMNH 5085 | PMNH 5086 | PMNH 5087 | PMNH 5088 | PMNH 5089 |
|---|---|---|---|---|---|---|---|---|
| **Sex** | Female | Male | Female | Female | Male | Male | Male | Male |
| **Age** | adult | adult | adult | adult | adult | adult | adult | adult |
| **Morphometry** | | | | | | | | |
| SVL | 48.6 | 55.3 | 52 | 55.5 | 57.6 | 57.8 | 55 | 60 |
| TL | 93.2 | 113.8 | 35.0 (br) | 86.3 (rg) | 119.1 | 117.5 | 114 | 79.9 (rg) |
| TL/SVL | 1.92 | 2.06 | ND | ND | 2.07 | 2.03 | 2.07 | ND |
| Lpil | 11.3 | 13.2 | 11.8 | 12.4 | 13.7 | 13.5 | 13.5 | 15 |
| HL | 11.2 | 13.2 | 12.1 | 12.9 | 13.8 | 13.3 | 13.8 | 14.8 |
| HW | 7 | 7.7 | 7 | 7.3 | 8.7 | 8.1 | 7.9 | 9.3 |
| HH | 5.1 | 6.2 | 5.2 | 5.4 | 6.2 | 6.4 | 6.2 | 7.2 |
| TrL | 24 | 26.5 | 26.2 | 29.1 | 26.5 | 26.4 | 27 | 27.7 |
| NL | 15.7 | 20.3 | 18.6 | 18.1 | 19.2 | 20.3 | 19.8 | 20.9 |
| SNL | 0.6 | 0.6 | 0.6 | 0.6 | 0.7 | 0.7 | 0.7 | 0.8 |
| FNL | 1.6 | 1.8 | 1.7 | 1.8 | 2.2 | 2 | 1.8 | 2.1 |
| FrL | 3.4 | 4.1 | 3.7 | 3.8 | 4 | 4 | 4.2 | 4.5 |
| PFL | 2.3 | 2.1 | 2.3 | 2.2 | 2.4 | 2.3 | 2.2 | 2.1 |
| PFW | 1.7 | 1.5 | 1.7 | 1.7 | 1.8 | 1.5 | 1.6 | 1.7 |
| FrW | 2.2 | 2.2 | 2.3 | 2.4 | 2.3 | 2.3 | 2.3 | 2.4 |

*.....continued on the next page*

**TABLE 2.** (Continued)

| **Voucher No.** | PMNH 5082 | PMNH 5083 | PMNH 5084 | PMNH 5085 | PMNH 5086 | PMNH 5087 | PMNH 5088 | PMNH 5089 |
|---|---|---|---|---|---|---|---|---|
| **Sex** | Female | Male | Female | Female | Male | Male | Male | Male |
| **Age** | adult | adult | adult | adult | adult | adult | adult | adult |
| FLL | 17.5 | 22 | 20 | 20.2 | 21 | 22.4 | 20.8 | 21 |
| HLL | 28.6 | 36.1 | 32.2 | 32.2 | 36.2 | 36 | 35.7 | 35.8 |
| HLL/SVL | 0.59 | 0.65 | 0.62 | 0.58 | 0.63 | 0.62 | 0.65 | 0.60 |
| HRL | 10.8 | 13.1 | 11.6 | 11.7 | 12.8 | 12.5 | 12 | 13 |
| FL | 9.3 | 11 | 9.8 | 9.5 | 10 | 10.8 | 10 | 11.2 |
| LFPR | 8.5 | 12 | 9.9 | 9.8 | 12 | 11 | 11.2 | 11.6 |
| LFPS | 1.6 | 1.4 | 2 | 1.8 | 1.6 | 1.8 | 1.8 | 2.4 |
| **Meristic** | | | | | | | | |
| DS | 56 | 53 | 52 | 54 | 53 | 54 | 56 | 52 |
| G | 26 | 27 | 26 | 27 | 29 | 27 | 27 | 28 |
| Coll | 10 | 9 | 10 | 9 | 8 | 11 | 8 | 10 |
| FP (r/l) | 18/19 | 16/18 | 17/17 | 16/16 | 18/18 | 18/18 | 16/17 | 16/15 |
| FPS | 4 | 4 | 4 | 3 | 2 | 3 | 3 | 4 |
| VL | 17 | 16 | 16 | 16 | 17 | 16 | 15 | 15 |
| VT | 38 | 35 | 36 | 36 | 36 | 35 | 34 | 33 |
| NCWS | 28 | 25 | 28 | 26 | 27 | 26 | 27 | 25 |
| SDLT 4th | 26 | 26 | 26 | 27 | 25 | 28 | 26 | 27 |
| SAT 4th | 4 | 4 | 4 | 4 | 4 | 4 | 4 | 4 |
| SDLF 4th | 20 | 19 | 20 | 19 | 21 | 18 | 18 | 19 |
| SqDors | 150 | 144 | 134 | 142 | 145 | 131 | 132 | 135 |
| SL (r/l) | 9/9 | 9/8 | 9/9 | 9/8 | 10/9 | 9/10 | 10/10 | 9/10 |
| SLAS (r/l) | 6/6 | 6/5 | 6/6 | 6/5 | 7/6 | 6/6 | 7/6 | 6/7 |
| IL (r/l) | 6/6 | 7/7 | 7/8 | 7/6 | 8/7 | 7/7 | 6/6 | 6/6 |
| Submax | 5 | 5 | 5 | 5 | 5 | 5 | 5 | 5 |
| Supracil (r/l) | 4/4 | 5/5 | 4/4 | 4/4 | 4/5 | 4/4 | 6/6 | 6/5 |
| **Categorical** | | | | | | | | |
| FMIL | + | + | + | + | + | + | + | + |
| SOM | + | + | + | + | + | + | + | + |
| FSO | - | - | - | - | - | - | - | - |
| INTR | - | - | - | - | - | - | - | - |
| Gran | + | + | + | + | + | + | + | + |
| LB | + | + | + | + | + | + | + | + |

## Identification

The occurrence of *E. fasciata* in Pakistan is confirmed here based on newly collected voucher specimens (Figs. 2 & 8), morphological comparison with genetically verified material from Iran examined by Orlova *et al.* (2023), and evidence from both mitochondrial and nuclear markers (Fig. 3). The Pakistani lizards agree with Iranian *E. fasciata* in their general morphology and coloration (see Table 2 & Appendix 2). Multivariate analysis of morphometric and meristic characters further supported their morphological assignment to *Eremias fasciata*, congruent with the molecular results (Figs. 1, 3-4). Analyses of the mitochondrial COI and cytochrome *b* markers consistently separate

the Pakistani specimens of *E. fasciata* from *E. chagaiensis* **sp. nov.** and place them with reference material identified as *E. fasciata*. This assignment is independently corroborated by the nuclear Rag-1 marker, for which DJ13825 represents a distinct *E. fasciata* allele separated from those detected in *E. chagaiensis* **sp. nov.** (Fig. 3).

### Distribution in Pakistan

The new material documents *E. fasciata* from several localities across western Balochistan. The eleven georeferenced Pakistani localities extend from 28.0210° to 29.3531° N and from 61.5442° to 63.0536° E, with a maximum straight-line distance of approximately 197 km between the most distant records (Fig. 2A,B). The species thus occurs across a substantial part of the desert region surrounding Nokkundi and extending southward and toward the Iranian and Afghan borders. These records currently represent the southeastern limit of the documented range. Geographically, the Pakistani records lie between previously documented populations in eastern Iran and southwestern Afghanistan, confirming the long-debated occurrence of the species in Pakistan.. The nearest genetically verified Iranian records are situated east of Zabol and in the Neatak sand dunes of Sistan and Baluchistan Province (Orlova *et al*. 2023). The closest of these lies approximately 171 km north of the westernmost Pakistani record. Voucher-based Afghan records are known from the Helmand–Kandahar region, including localities near Darweshan, Chah-i-Angir, Delaram, and Kandahar (Wagner *et al*. 2016; Jablonski & Masroor 2021), with the nearest available Afghan record situated approximately 209 km northeast of the easternmost Pakistani locality. The new records therefore reduce the previously documented geographical gap and support a transboundary distribution of *E. fasciata* across eastern Iran, western Pakistan, and southern Afghanistan. Based on the current data, they do not establish continuous occupancy across this entire region, because extensive intervening areas remain unsurveyed (Fig. 2A). In this context, the record reported by Khan (2006) from central Pakistan may represent a misidentification.

### Extent of occurrence and area of occupancy

Based on the eleven georeferenced localities currently available for *E. fasciata* from Pakistan, the extent of occurrence, calculated as a minimum convex polygon, is approximately 9,191 km². The area of occupancy, calculated using a standard 2 × 2 km grid, is 44 km², corresponding to eleven occupied grid cells. These values refer exclusively to the currently documented Pakistani distribution and should not be interpreted as range estimates for the species as a whole (Fig. 2A, B).

### Habitat

In western Balochistan, *E. fasciata* was recorded in open arid landscapes dominated by compact gravelly, stony, or mixed gravel–sand substrates. During our surveys, *E. fasciata* was not observed in the loose dune sands occupied by *E. chagaiensis* **sp. nov.** This corresponds to observations from Iran, where *E. fasciata* has been reported from desert plains with a broad range of substrate types, including sandy and gravelly surfaces, salt-encrusted hamada, loess-like silts, and alluvial deposits. Iranian records span an elevational range of approximately 450–1,700 m, supporting its interpretation as a relatively widespread and ecologically flexible desert species (Orlova *et al.* 2023).

### Remarks

The present records provide modern voucher- and sequence-based evidence for the occurrence of *E. fasciata* in Pakistan. They further demonstrate that the species is regionally distributed in western Balochistan rather than being represented by an isolated peripheral record. Its confirmed occurrence is biogeographically consistent with verified populations in adjacent parts of Iran and Afghanistan and clarifies the continuity of the regional faunal assemblage across the southeastern Iranian Plateau. However, the northern, eastern, and southern limits of its Pakistani distribution remain unknown and will require additional sampling across Chagai and neighbouring districts of Pakistan.

**Identification key to the Pakistani species of the genus *Eremias* (modified from Masroor *et al.* 2020a, 2022).**

1. Subocular bordering mouth . . . . . 2
- Subocular not bordering mouth . . . . . *E. acutirostris*
2. A complete row of lateral scales of the 4th toe forming a distinct fringe or comb on its entire length . . . . . 3
- Lateral scales of 4th toe not forming distinct fringe . . . . . 4
3. Row of femoral pores reaches well short of the knee; the median dark dorsal stripes in adults interrupted and form reticulate pattern . . . . . *E. scripta*
- Row of femoral pores reaches to knee; dorsal stripes without any sign of vermiculation . . . . . *E. cholistanica*
4. Body dorsum of adults and juveniles provided with 5–11 dark stripes, broader than interspaces, none of the stripes containing light ocelli or spots; stripes persistent in adults, but sometimes indistinct so that back appears almost uniform sandy; usually only single median collar scale distinctly larger than adjacent gulars . . . . . 5
- The dorsum of adults contains dark stripes that break up into spots (ocelli), broken lines, or vermiculations; several collar scales are usually distinctly larger than adjacent gulars. . . . . 6
5. 4th toe with two complete rows of subdigital scales and a complete row of sharply pointed lateral scales, i.e., a total of 4 scales counted around penultimate phalanx. . . . . *E. fasciata*
- 4th toe with one complete row of subdigital scales and a complete row of lateral scales, i.e., total of three scales counted around penultimate phalanx . . . . . *E. kakari*
6. Dorsal scales (DS) 68–80; gular scales (G) 19–24; dorsal scale rows (SqDors) 178–198; juveniles and adults with a vermiculate dorsal pattern . . . . . *E. chagaiensis* **sp. nov.**
- Juveniles and adults lacking the above combination of characters . . . . . 7
7. Adults with four more or less regular rows of disconnected dark spots on dorsum between dorsolateral broader dark stripes, the latter with white ocelli at the edges and within each stripe; infranasal in contact with the rostral . . . . . *E. rafiqi*
- Adults with seven light stripes on the neck, transforming into disconnected series of white ocelli edged with black; no dorsolateral dark stripes, an outer-most series of white and black ocelli starts behind the eyes on each side, onto tympanum and flanks above the forelimb and hindlimb insertion; infranasal not in contact with the rostral. . . . . *E. killasaifullahi*

## Discussion

Regional knowledge of the herpetofauna of Balochistan and adjoining parts of Iran and Afghanistan has historically been based largely on scattered expeditions, museum collections, and broad faunal syntheses (Minton 1966; Mertens 1969; Anderson 1999; Sindaco & Jeremčenko 2008; Wagner *et al.* 2016). Although these works established the fundamental distributional framework for the region, extensive areas of western Pakistan and southern Afghanistan remain represented by few records. More recent field surveys and molecular studies have revealed substantially greater diversity than was apparent from traditional morphology-based taxonomy. This is particularly evident among lacertid lizards, for which multilocus analyses of Pakistani populations recovered several deeply divergent evolutionary lineages and demonstrated that the existing taxonomy does not adequately reflect regional genetic diversity or evolutionary history (Khan *et al.* 2021; Jablonski *et al.* 2025).

The description of *E. chagaiensis* **sp. nov.** forms part of a broader pattern of recent discoveries from the arid landscapes of Balochistan. These include *E. kakari*, *E. killasaifullahi*, *E. rafiqi*, *Microgecko tanishpaensis* (Masroor *et al.* 2020a, b; 2022), as well as geographically restricted taxa such as *Laudakia melanura nasiri* and *Cyrtopodion rhodocauda* (Khan 2006), which remain genetically untested. Masroor *et al.* (2022) interpreted several recently described taxa as examples of local microendemism and noted that narrowly distributed reptile lineages occur throughout Iran, Pakistan, and Afghanistan, particularly among Lacertidae and Gekkonidae (cf. Rastegar-Pouyani *et al.* 2010; Nazarov *et al.* 2026). Most previously documented examples are associated with isolated valleys or mountain systems. *Eremias chagaiensis* **sp. nov.** extends this pattern to an ecologically distinct lowland desert environment, where suitable sandy substrates occur as discontinuous patches within a predominantly gravelly and rocky landscape.

The apparent geographical restriction of the new species is broadly consistent with the model of psammobiont diversification proposed by Orlova *et al.* (2023) for the Iranian Plateau. Individual dune systems are separated by extensive mountain, rocky, and gravel-dominated landscapes that may strongly restrict dispersal among populations associated with loose sand. Temporal changes in the distribution and connectivity of these sandy habitats may consequently promote independent differentiation within separate desert sectors. Although this model was developed primarily from populations in central Iran, the distribution of *E. chagaiensis* **sp. nov.** suggests that a comparable process may operate in the Registan–Chagai desert system at the southeastern margin of the Iranian Plateau.

Field observations support a strong association of *E. chagaiensis* **sp. nov.** with loose sandy substrates. The species was recorded on low dunes, sand sheets, and wind-deposited sandy patches but was not observed on surrounding gravel plains or rocky surfaces. These surrounding non-sandy substrates therefore appear to form the environmental matrix surrounding the occupied habitat rather than part of the habitat itself. Such substrate specialization may reduce dispersal among sandy patches even where straight-line distances are relatively small. The currently estimated extent of occurrence is therefore compatible with an apparently range-restricted psammobiont lineage, although the distribution, continuity, and functional connectivity of suitable sandy habitat remain insufficiently quantified.

The phylogenetic position of *E. chagaiensis* **sp. nov.** provides further insight into diversification within the *E. fasciata* species complex. Despite its external resemblance to the recently described Iranian species *E. graphica*, mitochondrial data recover the new species as the sister lineage of *E. fasciata*, although support for this relationship was moderate. The similarity to *E. graphica* involves both dorsal coloration and general habitat structure. The habitat reported for *E. graphica* consists of mobile dunes embedded within gravel-dominated landscapes, where individuals use vegetated microsites and excavate burrows beneath plants (Orlova *et al.* 2023). Because *E. chagaiensis* **sp. nov.** and *E. graphica* are not recovered as immediate sister taxa, their shared morphology and habitat association may partly reflect convergence under comparable psammophilous conditions rather than inheritance from a recent common ancestor.

The sister relationship between *E. chagaiensis* **sp. nov.** and *E. fasciata* is particularly notable because both species occur within the same broader regional landscape. Orlova *et al.* (2023) regarded *E. fasciata* as a comparatively widespread and eurytopic member of the complex and proposed that diversification among related lineages was associated with increasing specialization for particular sandy environments. The observed association of *E. chagaiensis* **sp. nov.** with loose sand, contrasted with the broader substrate use documented for *E. fasciata*, is consistent with fine-scale ecological differentiation between the two lineages. A comparable situation was reported for *E. pseudofasciata*, which occurs on isolated, weakly stabilized dunes in geographical proximity to *E. fasciata* (Orlova *et al.* 2023). These examples suggest that historical fragmentation of sandy habitats and contemporary substrate selection may jointly contribute to the origin and maintenance of diversity within the complex. However, niche partitioning between *E. chagaiensis* **sp. nov.** and *E. fasciata* remains a hypothesis that requires replicated habitat-use observations, quantitative substrate measurements, and comparative sampling of both species.

The present results also have broader taxonomic implications. Molecular studies have repeatedly demonstrated that external morphology and the traditional subgeneric classification of *Eremias* do not always correspond to evolutionary relationships. Khan *et al.* (2021) detected deeply divergent Pakistani lineages within morphologically defined taxa, while Khan *et al.* (2021) and Orlova *et al.* (2023) found that several traditional subgenera, including *Rhabderemias*, were not recovered as fully monophyletic. The evolutionary relationships of *E. chagaiensis* **sp. nov.** are therefore more appropriately interpreted within the phylogenetic framework of the *E. fasciata* species complex than through its traditional subgeneric assignment.

The morphological resemblance between *E. chagaiensis* **sp. nov.** and *E. graphica* illustrates the limitations of identification based on external appearance alone. In the absence of molecular data, the Pakistani specimens could have been assigned to the Iranian species, resulting in an erroneous national record and an artificial extension of its known range. However, the MFA based on morphological characters separates *E. chagaiensis* **sp. nov.** from both *E. graphica* and the sympatric *E. fasciata*, indicating that their differentiation becomes apparent when multiple characters are considered jointly. Conversely, genetically distinct lineages may remain overlooked under the names of morphologically similar and supposedly widespread taxa. This case therefore highlights the value of an integrative approach combining mitochondrial and nuclear data with multivariate morphology, habitat information, and detailed geographical sampling. Such an approach is particularly important for the poorly studied desert reptiles of Balochistan, where superficial morphological similarity may obscure evolutionary distinctness.

Incomplete geographical sampling remains an additional source of uncertainty. Fieldwork in western Balochistan is constrained by remoteness, security limitations, extreme temperatures, and the short daily activity periods of desert reptiles. Individuals resembling known species may consequently remain undetected or may not be collected systematically, particularly when they occur at low apparent densities or during narrow activity windows. The interaction between low sampling intensity and morphological similarity probably contributes to the persistent gap between documented and actual reptile diversity in the region. The extension of the known range of *E. kakari* from Pakistan into Afghanistan (Jablonski & Masroor 2021) also demonstrates that an apparently localized taxon does not necessarily represent a genuine microendemic. Transboundary sampling of reptiles between Afghanistan and

Pakistan is therefore essential for distinguishing genuine biogeographic patterns from sampling artefacts caused by incomplete exploration (Jablonski *et al.* 2021). Against this background, the records presented here bring the total number of species in the subgenus *Rhabderemias* to 12, five of which are now known from Pakistan, and thus increase the number of *Eremias* species recorded from Pakistan to eight.

*Eremias chagaiensis* **sp. nov.** is currently known from four localities in Balochistan and is provisionally interpreted as an apparently range-restricted psammobiont component of the Registan–Chagai desert fauna. However, suitable sandy environments extend into poorly surveyed southwestern Afghanistan, and the true geographical range may be larger than currently documented (Figs. 2, 7). The available data are also insufficient to quantify population trends, habitat fragmentation, or the intensity of potential threats. Future work should therefore focus on targeted surveys of adjoining Afghan sand systems, spatial mapping of suitable substrates, and population-level genomic sampling to determine whether populations associated with individual dune systems are geographically and genetically isolated.

## Acknowledgements

We are grateful for the support of Reko Diq Mining Company (RDMC), Digby Wells Environmental (DWE), Hagler Bailly Pakistan (HBP) and particularly Ashley Price of RDMC and Byron Bester of DWE for providing much-needed assistance. The collection efforts by Muhammad Shakil, Adnan Arif and Ghulam Murtaza of HBP and Ali Doost and Hafeez Shahi Baloch of RDMC and others during the fieldwork are greatly appreciated. We are grateful to Shabir Ali Amir, Riaz Ahmed and Jehanzeb Khan from Pakistan Museum of Natural History for extending their support during the field and museum work and Jana Poláková for her great assistance in the DNA laboratory. We also thank two reviewers for their comments and suggestions on the manuscript. DJ was supported by the Scientific Grant Agency of the Slovak Republic (VEGA 1/0391/25).

## References

Agarwal, I. & Ramakrishnan, U. (2017) A phylogeny of open-habitat lizards (Squamata: Lacertidae: *Ophisops*) supports the antiquity of Indian grassy biomes. *Journal of Biogeography*, 44, 2021–2032. https://doi.org/10.1111/jbi.12999

Agarwal, I., Khandekar, A., Ramakrishnan, U., Vyas, R. & Giri, V.B. (2018) Two new species of the *Ophisops microlepis* (Squamata: Lacertidae) complex from northwestern India with a key to Indian *Ophisops*. *Journal of Natural History*, 52 (13–16), 819–847. https://doi.org/10.1080/00222933.2018.1436203

Ali, A., Chen, D.L., Dujsebayeva, T.N., Song, Q., Terbish, K., Li, J., Qi, Y. & Guo, X.G. (2025) Phylogeography of a dominant desert lizard reveals the synergistic effects of topography and climate dynamics on diversification in arid eastern-Central Asia. *Zoological Research*, 46 (3), 485–504. https://doi.org/10.24272/j.issn.2095-8137.2024.327

Ananjeva, N.B., Borkin, L.Y., Darevsky, I.S. & Orlov, N.L. (1998) *Amphibians and Reptiles. Encyclopedia of Russian Nature*. ABF, Moscow, 574 pp. [in Russian]

Anderson, S.C. & Leviton, A.E. (1967) A new species of *Eremias* (Reptilia: Lacertidae) from Afghanistan. *Occasional Papers of the California Academy of Sciences*, 64, 1–4.

Anderson, S.C. (1999) *The Lizards of Iran. Contributions to Herpetology, Volume 15*. Society for the Study of Amphibians and Reptiles, Ithaca, New York, vii + 442 pp.

Arnold, E.N. (1986) The hemipenis of lacertid lizards (Reptilia: Lacertidae): structure, variation and systematic implications. *Journal of Natural History*, 20 (5), 1221–1257. https://doi.org/10.1080/00222938600770811

Arnold, E.N. (1989) Towards a phylogeny and biogeography of the Lacertidae: relationships within an Old-World family of lizards derived from morphology. *Bulletin of the British Museum (Natural History), Zoology*, 55 (2), 209–257.

Baig, K.J. & Masroor, R. (2006) A new species of *Eremias* (Sauria: Lacertidae) from Cholistan Desert, Pakistan. *Russian Journal of Herpetology*, 13 (3), 167–174. https://doi.org/10.30906/1026-2296-2006-13-3-167-174

Barabanov, A.V. (2009) *Aspidorhinus* Eichwald, 1841 as a valid subgeneric name for the *Eremias velox* species group (Sauria: Lacertidae). *Current Studies in Herpetology*, 9 (1–2), 59–61. [in Russian with English summary]

Başoğlu, M. & Hellmich, W. (1968) Eine neue Eremias-Form aus Ost-Anatolien (Reptilia: Lacertidae). *Ege Üniversitesi Fen Fakültesi İlmi Raporlar Serisi*, 67, 3–7.

Bedriaga, J. von (1907 [1905]) Neue Saurier aus Russisch-Asien. *Annuaire du Musée Zoologique de l'Académie Impériale des Sciences de St.-Pétersbourg*, 10, 210–243.
Bedriaga, J. von (1912) Amphibien und Reptilien. *In*: *Wissenschaftliche Resultate der von N.M. Przewalski nach Central-Asien unternommenen Reisen, Zoologischer Theil, Band III, Abtheilung 1, Teil 4*. Kaiserliche Akademie der Wissenschaften, St. Petersburg, pp. 503–769. [in Russian and German]
Bischoff, W. & Böhme, W. (1980) Der systematische Status der türkischen Wüstenrenner des Subgenus Eremias (Sauria: Lacertidae). *Zoologische Beiträge*, 26 (2), 297–306.
Böhme, W. & Szczerbak, N.N. (1991) Ein neuer Wüstenrenner aus dem Hochland Afghanistans, *Eremias* (*Eremias*) *afghanistanica* sp. n. (Reptilia: Sauria: Lacertidae). *Bonner zoologische Beiträge*, 42 (2), 137–141.
Boulenger, G.A. (1890) *The Fauna of British India, Including Ceylon and Burma. Reptilia and Batrachia*. Taylor & Francis, London, xviii + 541 pp.
https://doi.org/10.5962/bhl.title.100797
Boulenger, G.A. (1918) A synopsis of the lizards of the genus *Eremias*. *Journal of Zoological Research*, 3 (1), 1–12.
Boulenger, G.A. (1921) *Monograph of the Lacertidae. Vol. II*. Trustees of the British Museum (Natural History), London, viii + 451 pp.
https://doi.org/10.5962/bhl.title.54022
Chan, K.O. & Grismer, L.L. (2026) GroupStruct2: A User-Friendly Graphical User Interface for Statistical and Visual Support in Species Diagnosis. *Systematic Biology*, 75 (4), 814–823.
https://doi.org/10.1093/sysbio/syaf090
Chernomor, O., von Haeseler, A. & Minh, B.Q. (2016) Terrace-aware data structure for phylogenomic inference from supermatrices. *Systematic Biology*, 65 (6), 997–1008.
https://doi.org/10.1093/sysbio/syw037
Chirikova, M.A. (2004) Variability of *Eremias velox* Pallas, 1771 (Reptilia: Sauria) from Kazakhstan. *Selevinia*, 2004, 24–34. [in Russian]
Darevsky, I.S. & Szczerbak, N.N. (1978) *Eremias andersoni*, a new lizard (Reptilia: Lacertilia: Lacertidae) from Iran. *Journal of Herpetology*, 12 (1), 13–15.
https://doi.org/10.2307/1563496
de Queiroz, K. (2007) Species concepts and species delimitation. *Systematic Biology*, 56 (6), 879–886.
https://doi.org/10.1080/10635150701701083
Dufresnes, C., Poyarkov, N. & Jablonski, D. (2023) Acknowledging more biodiversity without more species. *Proceedings of the National Academy of Sciences of the United States of America*, 120 (40), e2302424120.
https://doi.org/10.1073/pnas.2302424120
Garcia-Porta, J., Irisarri, I., Kirchner, M., Rodríguez, A., Kirchhof, S., Brown, J.L., MacLeod, A., Turner, A.P., Ahmadzadeh, F., Albaladejo, G., Crnobrnja-Isailovic, J., De la Riva, I., Fawzi, A., Galán, P., Göçmen, B., Harris, D.J., Jiménez-Robles, O., Joger, U., Jovanović Glavaš, O., Karış, M., Koziel, G., Künzel, S., Lyra, M., Miles, D., Nogales, M., Oğuz, M.A., Pafilis, P., Rancilhac, L., Rodríguez, N., Rodríguez Concepción, B., Sanchez, E., Salvi, D., Slimani, T., S'khifa, A., Turk Qashqaei, A., Žagar, A., Lemmon, A., Lemmon, E.M., Carretero, M.A., Carranza, S., Philippe, H., Sinervo, B., Müller, J., Vences, M. & Wollenberg Valero, K.C. (2019) Environmental temperatures shape thermal physiology as well as diversification and genome-wide substitution rates in lizards. *Nature Communications*, 10, 4077.
https://doi.org/10.1038/s41467-019-11943-x
Gouy, M., Tannier, E., Comte, N. & Parsons, D.P. (2021) SeaView Version 5: a multiplatform software for multiple sequence alignment, molecular phylogenetic analyses, and tree reconciliation. *Methods in Molecular Biology*, 2231, 241–260.
https://doi.org/10.1007/978-1-0716-1036-7_15
Grismer, L.L. (2025) Introducing multiple factor analysis (MFA) as a diagnostic taxonomic tool complementing principal component analysis (PCA). *ZooKeys*, 1248, 93–109.
https://doi.org/10.3897/zookeys.1248.159516
Groth, J.G. & Barrowclough, G.F. (1999) Basal divergences in birds and the phylogenetic utility of the nuclear RAG-1 gene. *Molecular Phylogenetics and Evolution*, 12 (2), 115–123.
https://doi.org/10.1006/mpev.1998.0603
Guindon, S., Dufayard, J.-F., Lefort, V., Anisimova, M., Hordijk, W. & Gascuel, O. (2010) New algorithms and methods to estimate maximum-likelihood phylogenies: assessing the performance of PhyML 3.0. *Systematic Biology*, 59 (3), 307–321.
https://doi.org/10.1093/sysbio/syq010
Guo, X., Dai, X., Chen, D., Papenfuss, T.J., Ananjeva, N.B., Melnikov, D.A. & Wang, Y. (2011) Phylogeny and divergence times of some racerunner lizards (Lacertidae: *Eremias*) inferred from mitochondrial 16S rRNA gene segments. *Molecular Phylogenetics and Evolution*, 61 (2), 400–412.
https://doi.org/10.1016/j.ympev.2011.06.022
Guo, X.-G., Chen, D.-L., Wan, H.-F. & Wang, Y.-Z. (2010) Review of systematics of the racerunner lizard (Lacertidae: *Eremias*). *Sichuan Journal of Zoology*, 29 (4), 665–672. [in Chinese with English abstract]
Hoang, D.T., Chernomor, O., von Haeseler, A., Minh, B.Q. & Vinh, L.S. (2018) UFBoot2: improving the ultrafast bootstrap approximation. *Molecular Biology and Evolution*, 35 (2), 518–522.
https://doi.org/10.1093/molbev/msx281

Ivanova, N.V., Zemlak, T.S., Hanner, R.H. & Hebert, P.D.N. (2007) Universal primer cocktails for fish DNA barcoding. *Molecular Ecology Notes*, 7 (4), 544–548.
https://doi.org/10.1111/j.1471-8286.2007.01748.x

Jablonski, D. & Masroor, R. (2021) First record of *Eremias kakari* Masroor *et al*., 2020 (Squamata: Lacertidae) for Afghanistan. *Bonn zoological Bulletin*, 70 (1), 63–65.
https://doi.org/10.20363/BZB-2021.70.1.063

Jablonski, D., Basit, A., Farooqi, J., Masroor, R. & Böhme, W. (2021) Biodiversity research in a changing Afghanistan. *Science*, 372 (6549), 1402.
https://doi.org/10.1126/science.abj8118

Jablonski, D., Khan, M.A., Kehlmaier, C., Masroor, R., Nadeem, M.S. & Fritz, U. (2025) Contrasting genetic diversity in the genus *Acanthodactylus* (Squamata: Lacertidae) at its eastern distribution edge. *Amphibia-Reptilia*, 46 (2), 207–226.
https://doi.org/10.1163/15685381-bja10216

Kalyaanamoorthy, S., Minh, B.Q., Wong, T.K.F., von Haeseler, A. & Jermiin, L.S. (2017) ModelFinder: fast model selection for accurate phylogenetic estimates. *Nature Methods*, 14 (6), 587–589.
https://doi.org/10.1038/nmeth.4285

Kessler, K.F. (1878) Puteshestvie po Zakavkazskomu krayu v 1875 godu s zoologicheskoyu tsel'yu [A journey through the Transcaucasian region in 1875 for zoological purposes]. *Trudy Sankt-Peterburgskogo Obshchestva Estestvoispytatelei*, 8 (Supplement), 1–200. [in Russian]

Khan, M.A., Jablonski, D., Nadeem, M.S., Masroor, R., Kehlmaier, C., Spitzweg, C. & Fritz, U. (2021) Molecular phylogeny of *Eremias* spp. from Pakistan contributes to a better understanding of the diversity of racerunners. *Journal of Zoological Systematics and Evolutionary Research*, 59, 466–483.
https://doi.org/10.1111/jzs.12426

Khan, M.S. & Ahmed, N. (1987) On a collection of amphibians and reptiles from Baluchistan, Pakistan. *Pakistan Journal of Zoology*, 19 (4), 361–370.

Khan, M.S. (2006) *Amphibians and Reptiles of Pakistan*. Krieger Publishing Company, Malabar, Florida, 311 pp.

Kyriazi, P., Poulakakis, N., Parmakelis, A., Crochet, P.A., Moravec, J., Rastegar-Pouyani, N., Tsigenopoulos, C.S., Magoulas, A., Mylonas, M. & Lymberakis, P. (2008) Mitochondrial DNA reveals the genealogical history of the snake-eyed lizards (*Ophisops elegans* and *O. occidentalis*) (Sauria: Lacertidae). *Molecular Phylogenetics and Evolution*, 49 (3), 795–805.
https://doi.org/10.1016/j.ympev.2008.08.021

Lantz, L.A. (1928) Les *Eremias* de l'Asie occidentale. *Bulletin du Musée de Géorgie*, 4, 1–72; 5, 1–64, pls. 1–3.

Masroor, R., Khan, M.A., Nadeem, M.S., Amir, S.A., Khisroon, M. & Jablonski, D. (2022) Appearances often deceive in racerunners: integrative approach reveals two new species of *Eremias* (Squamata: Lacertidae) from Pakistan. *Zootaxa*, 5175 (1), 55–87.
https://doi.org/10.11646/zootaxa.5175.1.3

Masroor, R., Khisroon, M., Khan, M.A. & Jablonski, D. (2020a) A new species of *Eremias* Fitzinger, 1834 (Squamata: Lacertidae) from the arid mountains of Pakistan. *Zootaxa*, 4786 (1), 101–121.
https://doi.org/10.11646/zootaxa.4786.1.8

Masroor, R., Khisroon, M., Khan, M.A. & Jablonski, D. (2020b) A new species of *Microgecko* Nikolsky, 1907 (Squamata: Gekkonidae) from Pakistan. *Zootaxa*, 4780 (1), 147–164.
https://doi.org/10.11646/zootaxa.4780.1.7

Mertens, R. (1969) Die Amphibien und Reptilien West-Pakistans. *Stuttgarter Beiträge zur Naturkunde*, 197, 1–96.

Minton, S.A. (1966) A contribution to the herpetology of West Pakistan. *Bulletin of the American Museum of Natural History*, 134 (2), 29–184.

Moravec, J. (1994) A new lizard from Iran, *Eremias* (*Eremias*) *lalezharica* sp. n. (Reptilia: Lacertilia: Lacertidae). *Bonner zoologische Beiträge*, 45 (1), 61–66.

Mozaffari, O., Ahmadzadeh, F. & Parham, J.F. (2011) *Eremias papenfussi* sp. nov., a new lacertid lizard (Sauria: Lacertidae) from Tehran Province, Iran. *Zootaxa*, 3114 (1), 57–62.
https://doi.org/10.11646/zootaxa.3114.1.6

Mozaffari, O., Ahmadzadeh, F. & Saberi-Pirooz, R. (2020) Fahimi's racerunner, a new species of the genus *Eremias* Fitzinger, 1834 (Sauria: Lacertidae) from Iran. *Zootaxa*, 4768 (4), 565–578.
https://doi.org/10.11646/zootaxa.4768.4.7

Nazarov, R.A., Nabizadeh, H., Rajabizadeh, M., Moaddab, M., Nikolaev, O.D., Solovyeva, E.N., Melnikov, D.A., Ananjeva, N.B., Poyarkov, N.A. & Ratsegar-Pouyani, E. (2026) Taxonomic diversity of Iranian thin-toed geckos of the *Cyrtopodion agamuroides–gastropholis* species complex (Reptilia: Squamata: Gekkonidae) with description of ten new species. *Russian Journal of Herpetology*, 33 (2), 85–168.
https://doi.org/10.30906/1026-2296-2026-33-2-85-168

Nikolsky, A.M. (1896) Diagnoses reptilium et amphibiorum novorum in Persia orientali a N. Zarudny collectorum. *Annuaire du Musée Zoologique de l'Académie Impériale des Sciences de St.-Pétersbourg*, 1, 369–372.

Nikolsky, A.M. (1915) *Fauna Rossii i sopredel'nykh stran. Presmykayushchiesya (Reptilia). Vol. I. Chelonia and Sauria*. Imperial Academy of Sciences, Petrograd, 532 pp. [in Russian]

Olson, D.M., Dinerstein, E., Wikramanayake, E.D., Burgess, N.D., Powell, G.V.N., Underwood, E.C., D'Amico, J.A., Itoua, I., Strand, H.E., Morrison, J.C., Loucks, C.J., Allnutt, T.F., Ricketts, T.H., Kura, Y., Lamoreux, J.F., Wettengel, W.W., Hedao,

P. & Kassem, K.R. (2001) Terrestrial ecoregions of the world: a new map of life on Earth. *BioScience*, 51 (11), 933–938. https://doi.org/10.1641/0006-3568(2001)051[0933:TEOTWA]2.0.CO;2

Orlova, V.F., Poyarkov, N.A. Jr., Chirikova, M.A., Nazarov, R.A., Munkhbaatar, M., Munkhbayar, K. & Terbish, K. (2017) MtDNA differentiation and taxonomy of Central Asian racerunners of the *Eremias multiocellata–E. przewalskii* species complex (Squamata: Lacertidae). *Zootaxa*, 4282 (1), 1–42. https://doi.org/10.11646/zootaxa.4282.1.1

Orlova, V.F., Rasegar-Pouyani, E., Rajabizadeh, K., Nabizadeh, H., Poyarkov, N.A., Melnikov, D.A. & Nazarov, R.A. (2023) Taxonomic diversity of racerunners with descriptions of two new *Eremias* species (Sauria: Lacertidae) from Central Iran. *Zootaxa*, 5369 (3), 336–368. https://doi.org/10.11646/zootaxa.5369.3.2

Pavlicev, M. & Mayer, W. (2009) Fast radiation of the subfamily Lacertinae (Reptilia: Lacertidae): history or methodical artefact? *Molecular Phylogenetics and Evolution*, 52 (3), 727–734. https://doi.org/10.1016/j.ympev.2009.04.020

QGIS Development Team (2025) QGIS Geographic Information System, Version 3.44.0 'Solothurn'. Open Source Geospatial Foundation Project. Available from: https://qgis.org (accessed 27 June 2025)

Rambaut, A., Drummond, A.J., Xie, D., Baele, G. & Suchard, M.A. (2018) Posterior Summarization in Bayesian Phylogenetics Using Tracer 1.7. *Systematic Biology*, 67 (5), 901–904. https://doi.org/10.1093/sysbio/syy032

Rastegar-Pouyani, E., Hosseinian, S., Rafiee, S., Kami, H.G., Rajabizadeh, M. & Wink, M. (2016) A new species of the genus *Eremias* Fitzinger, 1834 (Squamata: Lacertidae) from Central Iran, supported by mtDNA sequences and morphology. *Zootaxa*, 4132 (2), 207–220. https://doi.org/10.11646/zootaxa.4132.2.2

Rastegar-Pouyani, E., Rastegar-Pouyani, N., Kazemi Noureini, S., Joger, U. & Wink, M. (2010) Molecular phylogeny of the *Eremias persica* complex of the Iranian Plateau (Reptilia: Lacertidae), based on mtDNA sequences. *Zoological Journal of the Linnean Society*, 158 (3), 641–660. https://doi.org/10.1111/j.1096-3642.2009.00553.x

Rastegar-Pouyani, N. & Nilson, G. (1997) A new species of *Eremias* (Sauria: Lacertidae) from Fars Province, South-Central Iran. *Russian Journal of Herpetology*, 4 (2), 94–101. https://doi.org/10.30906/1026-2296-1997-4-2-94-101

Rastegar-Pouyani, N. & Rastegar-Pouyani, E. (2001) A new species of *Eremias* (Sauria: Lacertidae) from highlands of Kermanshah Province, western Iran. *Asiatic Herpetological Research*, 9, 107–112. https://doi.org/10.5962/bhl.part.15563

Rastegar-Pouyani, E., Hosseinian Yousefkhani, S.S. & Wink, M. (2015) Taxonomic reevaluation of *Eremias strauchi strauchi* Kessler, 1878 and *Eremias strauchi kopetdaghica* Szczerbak, 1972, based on nuclear and mitochondrial DNA sequences (Reptilia: Lacertidae). *Zoology in the Middle East*, 61 (2), 118–124. https://doi.org/10.1080/09397140.2015.1020615

Ronquist, F., Teslenko, M., van der Mark, P., Ayres, D.L., Darling, A., Höhna, S., Larget, B., Liu, L., Suchard, M.A. & Huelsenbeck, J.P. (2012) MrBayes 3.2: Efficient Bayesian phylogenetic inference and model choice across a large model space. *Systematic Biology*, 61, 539–542. https://doi.org/10.1093/sysbio/sys029

Rozas, J., Ferrer-Mata, A., Sánchez-del Barrio, J.C., Guirao-Rico, S., Librado, P., Ramos-Onsins, S.E. & Sánchez-Gracia, A. (2017) DnaSP 6: DNA sequence polymorphism analysis of large data sets. *Molecular Biology and Evolution*, 34 (12), 3299–3302. https://doi.org/10.1093/molbev/msx248

Sindaco, R. & Jeremčenko, V.K. (2008) *The Reptiles of the Western Palearctic. Vol. 1. Annotated Checklist and Distributional Atlas of the Turtles, Crocodiles, Amphisbaenians and Lizards of Europe, North Africa, Middle East and Central Asia*. Edizioni Belvedere, Latina, 579 pp.

Smith, M.A. (1935) *The Fauna of British India, Including Ceylon and Burma. Reptilia and Amphibia. Vol. II—Sauria*. Taylor & Francis, London, xiii + 440 pp.

Stephens, M., Smith, N.J. & Donnelly, P. (2001) A new statistical method for haplotype reconstruction from population data. *The American Journal of Human Genetics*, 68 (4), 978–989. https://doi.org/10.1086/319501

Szczerbak, N.N. (1971) Taxonomy of the genus *Eremias* (Sauria: Reptilia) in connection with the centres of development of the desert-steppe fauna in the Palaearctic. *Vestnik Zoologii*, 1971 (2), 48–55. [in Russian]

Szczerbak, N.N. (1972) A new subspecies of *Eremias strauchi—Eremias strauchi kopetdaghica* ssp. nova (Sauria: Reptilia) from Turkmenia. *Vestnik Zoologii*, 1972 (6), 83–86. [in Russian]

Szczerbak, N.N. (1974) *Racerunners of the Palaearctic*. Naukova Dumka, Kiev, 296 pp. [in Russian]

Szczerbak, N.N. (1981) *Eremias velox* (Pallas, 1771)—Schneller Wüstenrenner. *In*: Böhme, W. (Ed.), *Handbuch der Reptilien und Amphibien Europas. Band 1/I, Echsen I*. Akademische Verlagsgesellschaft, Wiesbaden, pp. 447–460.

Tian, L. & Guo, X. (2022) Complete mitochondrial genomes of five racerunners (Lacertidae: *Eremias*) and comparison with other lacertids: insights into the structure and evolution of the control region. *Genes*, 13 (5), 726. https://doi.org/10.3390/genes13050726

Tian, L., Xu, R., Chen, D., Ananjeva, N.B., Brown, R.M., Min, M.S., Cai, B., Mijidsuren, B., Zhang, B. & Guo, X. (2024) Range-wide phylogeography and ecological niche modeling provide insights into the evolutionary history of the Mongolian racerunner (*Eremias argus*) in Northeast Asia. *Animals*, 14 (7), 1124. https://doi.org/10.3390/ani14071124

Townsend, T.M., Larson, A., Louis, E. & Macey, J.R. (2004) Molecular phylogenetics of Squamata: the position of snakes, amphisbaenians, and dibamids, and the root of the squamate tree. *Systematic Biology*, 53 (5), 735–757. https://doi.org/10.1080/10635150490522340

Uetz, P., Freed, P., Aguilar, R., Reyes, F., Kudera, J. & Hošek, J. (Eds.) (2026) *The Reptile Database*. Available from: https://www.reptile-database.org (accessed 5 May 2026)

Vasconcelos, R., Montero-Mendieta, S., Simó-Riudalbas, M., Sindaco, R., Santos, X., Fasola, M., Llorente, G., Razzetti, E. & Carranza, S. (2016) Unexpectedly high levels of cryptic diversity uncovered by a complete DNA barcoding of reptiles of the Socotra Archipelago. *PLoS ONE*, 11 (3), e0149985. https://doi.org/10.1371/journal.pone.0149985

Vences, M., Miralles, A. & Dufresnes, C. (2024a) Next-generation species delimitation and taxonomy: implications for biogeography. *Journal of Biogeography*, 51, 1709–1722. https://doi.org/10.1111/jbi.14807

Vences, M., Patmanidis, S., Schmidt, J.-C., Matschiner, M., Miralles, A. & Renner, S.S. (2024b) Hapsolutely: a user-friendly tool integrating haplotype phasing, network construction, and haploweb calculation. *Bioinformatics Advances*, 4 (1), vbae083. https://doi.org/10.1093/bioadv/vbae083

Wagner, P., Bauer, A.M., Leviton, A.E., Wilms, T.M. & Böhme, W. (2016) A checklist of the amphibians and reptiles of Afghanistan: exploring herpetodiversity using biodiversity archives. *Proceedings of the California Academy of Sciences*, Series 4, 63 (13), 457–565.

Wong, T.K.F., Ly-Trong, N., Ren, H., Demotte, P., Baños, H., Roger, A.J., Susko, E., Bielow, C., De Maio, N., Goldman, N., Hahn, M.W., dos Reis, M., Vinh, L.S., Huttley, G., Lanfear, R. & Minh, B.Q. (2026) IQ-TREE 3: phylogenomic inference software using complex evolutionary models. *Molecular Biology and Evolution*, 43 (5), msag117. https://doi.org/10.1093/molbev/msag117

Zhou, T., Liu, J. & Guo, X. (2016) Complete mitogenome of a variegated racerunner, *Eremias vermiculata*, from north of Tianshan Mountains, Xinjiang, China. *Mitochondrial DNA Part A*, 27 (4), 2765–2766. https://doi.org/10.3109/19401736.2015.1053055

**Appendix 1.** Sequence data used in phylogenetic analyses. Published sequences are listed by GenBank accession number.

| Taxon | GenBank accession(s) / voucher(s) | Source |
|---|---|---|
| **COI (n = 107)** | | |
| *Eremias acutirostris* | MT524255.1, MT524258.1 | Khan *et al.* (2021) |
| *Eremias andersoni* | OR268252.1-OR268258.1 | Orlova *et al.* (2023) |
| *Eremias chagaiensis* **sp. nov.** | PZ987601.1, PZ987603.1–PZ987611.1 | This study |
| *Eremias cholistanica* | MT524253.1, MT524254.1 | Khan *et al.* (2021) |
| *Eremias fasciata* | OR268267.1-OR268283.1; PZ987599.1–PZ987600.1, PZ987602.1 | Orlova *et al.* (2023); this study |
| *Eremias* cf. *fasciata* | OR268285.1 | Orlova *et al.* (2023) |
| *Eremias graphica* | OR268242.1-OR268251.1 | Orlova *et al.* (2023) |
| *Eremias kakari* | MT524248.1, MT524256.1 | Khan *et al.* (2021) |
| *Eremias kavirensis* | OR268284.1 | Orlova *et al.* (2023) |
| *Eremias lasdini* | OR268308.1-OR268310.1 | Orlova *et al.* (2023) |
| *Eremias lineolata* | OR268286.1-OR268300.1; OR268302.1-OR268306.1 | Orlova *et al.* (2023) |
| *Eremias pleskei* | OR268319.1-OR268324.1 | Orlova *et al.* (2023) |
| *Eremias pseudofasciata* | OR268259.1-OR268266.1 | Orlova *et al.* (2023) |
| *Eremias rafiqi* | MT524249.1 | Khan *et al.* (2021) sensu Masroor *et al.* (2022) |
| *Eremias scripta* | OR268301.1; OR268311.1-OR268318.1 | Orlova *et al.* (2023) |
| *Eremias vermiculata* | OR268307.1 | Orlova *et al.* (2023) |
| **Outgroup** | | |
| *Acanthodactylus boskianus* | MN015076.1 | Garcia-Porta *et al.* (2019) |
| *Lacerta agilis* | CM020436.1 | Gemmell *et al.*, unpublished |
| *Mesalina balfouri* | KU567487.1 | Vasconcelos *et al.* (2016) |
| *Ophisops elegans* | EU081525.1 | Kyriazi *et al.* (2008) |
| **cyt b (n = 25)** | | |
| *Eremias acutirostris* | MT554471.1 | Khan *et al.* (2021) |
| *Eremias argus* | OR019626.1 | Tian *et al.* (2024) |
| *Eremias arguta* | MK831336.1 | Gong *et al.*, unpublished |
| *Eremias chagaiensis* **sp. nov.** | QB002729-QB002738.1 | This study |
| *Eremias cholistanica* | MT554472.1 | Khan *et al.* (2021) |
| *Eremias fasciata* | QB002726-QB002728.1 | This study |
| *Eremias killasaifullahi* | MT554459.1 | Khan *et al.* (2021) |
| *Eremias kopetdaghica* | KJ468076.1 | Rastegar-Pouyani *et al.* (2015) |
| *Eremias rafiqi* | MT554454.1 | Khan *et al.* (2021) sensu Masroor *et al.* (2022) |
| *Eremias scripta* | OM935765.1 | Tian & Guo (2022) |
| *Eremias vermiculata* | PQ311658.1; KP981389.1 | Ali *et al.* (2025); Zhou *et al.* (2016) |
| **Outgroup** | | |
| *Acanthodactylus blanfordii* | PQ867993.1 | Jablonski *et al.* (2025) |
| *Lacerta agilis* | CM020436.1 | Gemmell *et al.*, unpublished |
| **Rag-1 (n = 9)** | | |
| *Eremias chagaiensis* **sp. nov.** | QB002365-QB002371.1 | This study |
| *Eremias fasciata* | QB002372.1 | This study |
| *Eremias scripta* | AY662615.1 | Townsend *et al.* (2004) |

**APPENDIX 2.** Comparison of morphological characters of *Eremias* (*Rhabderemias*) *chagaiensis* **sp. nov.** with other species of the subgenus *Rhabderemias*, except *E. lasdini*. See material and methods section for abbreviation of characters (N/A= data not available, + = in contact, - = separated). For *E. fasciata*, morphological ranges combine published data with measurements of eight Pakistani specimens (PMNH 5082–5089) examined in this study. The number of specimens underlying the historical data is not available.

| Species name | **Source** | **Number of specimens** | **Max. SVL in mm** | **DS** | **VL** | **VT** | **G** | **NCWS** | **SAT 4th** | **SDLT 4th** | **FP** | **FPS** | **SOM** | **Dorsal color pattern of adult** | **Distribution** |
|---|---|---|---|---|---|---|---|---|---|---|---|---|---|---|---|
| *E. chagaiensis* **sp. nov.** | This study | 8 | 57.0 | 68–80 | 12–14 | 32–35 | 19–24 | 29–35 | 4 | 27–31 | 10–15 | 2–4 | + | vermiculate | NW & W Balochistan, Pakistan; possible in broad region of Registan desert of Afghanistan |
| *E. graphica* | Orlova *et al.* (2023) | 10 | 58.3 | 59–65 | 14–18 | 32–35 | 26–31 | 23–29 | NA | 22–29 | 15–18 | 4–6 | + | vermiculate | Central Iran (Tabas region); known from the type locality |
| *E. pseudofasciata* | Orlova *et al.* (2023) | 12 | 57.0 | 44–51 | 13–16 | 31–34 | 26–33 | 21–26 | NA | 24–31 | 14–19 | 3–7 | + | striped | Central–eastern Iran (Khorasan Province, Boshruiyeh region) |
| *E. kakari* | Masroor *et al.* (2020a) | 13 | 52.2 | 48–55 | 11–14 | 28–32 | 21–25 | 17–21 | 3 | 22–26 | 17–21 | 4–5 | + | striped | NW Balochistan, Pakistan and SE Afghanistan |
| *E. andersoni* | Darevsky & Szczerbak (1978) | 3 | 40.0 | 56–58 | 13–14 | 28–29 | 28–30 | 26–28 | 3 | 32 | 15–16 | NA | + | striped | NE Iran; only from the type locality |

*.....continued on the next page*

**APPENDIX 2.** (Continued)

| Species name | Source | Number of specimens | Max. SVL in mm | DS | VL | VT | G | NCWS | SAT 4th | SDLT 4th | FP | FPS | SOM | Dorsal color pattern of adult | Distribution |
|---|---|---|---|---|---|---|---|---|---|---|---|---|---|---|---|
| *E. cholistanica* | Baig & Masroor (2006) | 26 | 53.0 | 51–63 | 13–15 | 30–36 | 20–24 | 27–35 | 4 | 23–30 | 14–18 | 2–4 | + | striped | E Pakistan (Cholistan Desert, Punjab) |
| *E. fasciata* | Nikolsky (1915); Anderson (1999); Baig & Masroor (2006); This study | 8 + literature data (n unspecified) | 65.0 | 44–56 | 14–17 | 29–38 | 21–30 | 25–36 | 4 | 25–30 | 15–19 | 2–4 | + | striped | E Iran, SW Afghanistan, NW Balochistan, Pakistan |
| *E. lineolata* | Boulenger (1921); Lantz (1928); Anderson (1999); Baig & Masroor (2006) | NA | 55.0 | 54–62 (Boulenger 1921) | 12–14 | 26–35 | 18–30; 21–26 (Lantz, 1928) | 12–17 | 3 | NA | 9–17 | NA | + | striped | Turkmenistan, Uzbekistan, Tajikistan, S Kazakhstan, NE Iran, NW Afghanistan |
| *E. scripta* | Masroor *et al.* (2020a) | NA | 66.0 | 55–69 | 14–16 | 25–33 | 15–23 | 17–28 | 4 | NA | 12–13 | NA | + | striped | S Kazakhstan, Turkmenistan, NE Iran, Afghanistan, SW Pakistan, SE Uzbekistan, SW Tajikistan, Kyrgyzstan |
| *E. pleskei* | Nikolsky (1915); Anderson (1999) | NA | 60.0 | 48–63 | NA | 28–35 | 25–31 | 20–32 | NA | NA | 7–15 | 6–8 | + | striped | NW Iran, Armenia, Azerbaijan, NE Turkey |
| *E. vermiculata* | Bedriaga (1912); Boulenger (1921) | NA | 65.0 | 55–68; 59–71 (Bedriaga, 1912) | 18–20 | 36–38; 35–39 (Bedriaga, 1912) | 38–39; 31–43 (Bedriaga, 1912) | 42–46 | 3 | 24–26 | 20–23; 17–24 (Bedriaga, 1912) | NA | + | Striped and vermiculate | Mongolia, NW China, SE Kazakhstan |